FLEXURAL WAVES IN ELASTIC CIRCULAR PLATES BY METHOD OF CHARACTERISTICS

Pei Chi Chou

Herbert Abraham Koenig

Final Report

August 1965

(Also as DIT Report No. 160-6)

Prepared under Contract No. NsG-270-63

DREXEL INSTITUTE OF TECHNOLOGY

Philadelphia, Pennsylvania

NATIONAL AERONAUTICS AND SPACE ADMINISTRATION

TABLE OF CONTENTS

SUMMARY

16071

The Uflyand-Mindlin plate equations in the form of two second order equations in terms of plate-displacements are analyzed by the method of characteristics for the case of an infinite plate with a circular hole. Procedures of numerical integration along the four characteristic directions including the technique of handling the propagation of discontinuities, are established. Numerical examples presented include the cases of transverse shear and radial bending moments applied at the hole. The numerical accuracy obtained is satisfactory for most of the cases.

Author

SYMBOLS

A = arbitrary constant

B = arbitrary constant

c_p = plate velocity = $\sqrt{E/\rho(1-\nu^2)}$

c_2 = shear wave velocity = $\sqrt{G/\rho}$ = $\sqrt{E/2\rho(1+\nu)}$

D = flexural rigidity = $Eh^3/12(1-\nu^2)$

E = Modulus of Elasticity

G = shear modulus = $E/2(1+\nu)$

h = plate thickness

k = time for a ramp to reach its maximum value

k_2^2 = shear correction factor

M_r = radial bending moment

M_θ = tangential bending moment

Q_r = transverse shear stress resultant

r = radial distance

r_o = inner radius of plate

t = time

w = transverse displacement of the midplane

θ = tangential direction

ν = Poisson's ratio

ρ = density

ϕ = rotation of the cross-section about the tangential axis

Subscripts r and t designate partial differentiations (except Q_r and M_r)

ACKNOWLEDGMENT

The authors are indebted to Mr. Gordon Smith of the Lewis Research Center, NASA, for his guidance and encouragement in the course of this research.

We would like also to thank Professor N. Pagano and Mr. R. Mortimer for their stimulating discussions and critical comments.

I. INTRODUCTION

The research reported herein was motivated by the desire to understand the response of the structural wall of fuel tanks of space vehicles when impacted by meteoroids. After entering the fuel tank, a meteoroid could create a high-pressure region in the liquid fuel, capable of bursting the tank and causing catastrophic failure. The tank wall will be treated here as a large plate with a circular hole, under an axisymmetrical moving load. For simplicity, only linear plate equations will be used. In the present report, only a concentrated ring load will be considered. Currently, the case of arbitrarily distributed loads which vary with respect to time is being studied and the results will be reported at a later date.

The classical Lagrange's equation for flexural motions of elastic plates is parabolic in nature. According to this equation, the wave velocity of sinusoidal waves is inversely proportional to the wave length. For sharp transient inputs which excite waves of very short length, the wave propagation velocity approaches infinity and any suddenly applied disturbances are felt immediately at an infinite distance away. This is contradictory to experimental evidences.

By introducing correction terms due to rotatory inertia and shear effect, Uflyand [1] and Mindlin [2] derived a set of governing equations which are hyperbolic. Mindlin also showed that this set of equations may be deduced directly from the three-dimensional equations of elasticity. The theory behind these plate equations is analogous to the Timoshenko beam theory, which also includes the effects of shear force and rotatory inertia. Although it is more

realistic as compared to the classical Lagrange theory, the Uflyand-Mindlin theory is still approximate, since it involves the assumption of plane sections remaining plane, and the selection of a constant appearing in the relation between average transverse shear stress and strain. This theory gives accurate results for moderately short wave length and moderately high frequency inputs, but it cannot be considered accurate for very short waves.

Solutions of the Uflyand-Mindlin equations due to suddenly applied concentrated transverse loads were obtained by Miklowitz [3] and Lubkin [4]. Both of them used the Laplace transform method and after lengthy inversion processes, their results were in the form of quadratures with integrands containing different combinations of Bessel functions. To evaluate these results, numerical integration had to be performed on the electronic computer. Of importance, also, is the fact that their results can be extended only to inputs involving other time functions of transverse shear (convolution technique) and not to other types of inputs, such as suddenly applied moments.

Due to the hyperbolic nature of the governing equations, the method of characteristics may be used to find the solution. Following an analogous approach by Leonard and Budiansky [5], Jahsman [6] applied the method of characteristics to the flexural equations of Uflyand and Mindlin. He derived the physical characteristics, the characteristic equations and the relations which govern the propagation of jumps at the wave front, but he did not solve the characteristic equations behind the wave fronts. Jahsman used Mindlin's "plate-stress components" and "plate-displacement components" as the dependent variables, therefore his governing equations are first order differential equations consisting

of the plate-stress equations of motion and the plate-stress-displacement equations. In the present report, the axisymmetrical case is considered and the method of characteristics is applied to the two second order plate equations of motion in terms of the two plate-displacement components ϕ and w. These results are compared with those obtained by Jahsman.

The characteristic equations are then written in finite-difference form and a scheme is developed to solve these equations numerically for various inputs at the circular hole of an infinite plate. In particular, in solving the problem with an input in transverse shear Q_r, a special technique is introduced to handle the discontinuities along the steeper wave front in a four-wave system. A few numerical examples are presented.

II. Characteristic Equations

The Uflyand-Mindlin equations in polar coordinates for an elastic plate (with no surface tractions) under axisymmetrical loading conditions are

$$\frac{\partial M_r}{\partial r} + \frac{1}{r}(M_r - M_\theta) - Q_r = \frac{\rho h^3}{12}\frac{\partial^2 \phi}{\partial t^2} \tag{1}$$

$$\frac{\partial Q_r}{\partial r} + \frac{1}{r} Q_r = \rho h \frac{\partial^2 w}{\partial t^2} \tag{2}$$

$$M_r = D\left[\frac{\partial \phi}{\partial r} + \frac{\nu}{r}\phi\right] \tag{3}$$

$$M_\theta = D\left[\frac{\phi}{r} + \nu\frac{\partial \phi}{\partial r}\right] \tag{4}$$

$$Q_r = k_2^2 G h\left[\phi + \frac{\partial w}{\partial r}\right] \tag{5}$$

These equations are identical with (3) and (4) of [6], with $M_{r\theta} = Q_\theta = \partial/\partial\theta = 0$. They may also be transformed into (2) of [3]. The system of equations (1) to (5), which will be considered as the stress-displacement approach, are hyperbolic equations and their characteristic directions and characteristic equations have been derived by Jahsman [6]. In this report, we shall follow the displacement approach which uses a system of two second-order equations involving ϕ and w. The method of characteristics is applied to these two second-order equations. Substituting (3), (4), and (5) into (1) and (2) we have

$$\frac{\partial^2 \phi}{\partial r^2} - \frac{\rho h^3}{12D}\frac{\partial^2 \phi}{\partial t^2} = \frac{k_2^2 G h}{D}\left(\phi + \frac{\partial w}{\partial r}\right) + \frac{1}{r^2}\phi - \frac{1}{r}\frac{\partial \phi}{\partial r} \tag{6}$$

$$\frac{\partial^2 w}{\partial r^2} - \frac{\rho}{k_2^2 G}\frac{\partial^2 w}{\partial t^2} = -\frac{1}{r}\left(\phi + \frac{\partial w}{\partial r}\right) - \frac{\partial \phi}{\partial r} \tag{7}$$

These two equations are also hyperbolic and their physical characteristics, or characteristic directions, are

$$\left.\begin{matrix} I^+ \\ I^- \end{matrix}\right\} \quad \frac{dr}{dt} = \pm c_p \tag{8}$$

$$\left.\begin{matrix} II^+ \\ II^- \end{matrix}\right\} \quad \frac{dr}{dt} = \pm k_2 c_2 \tag{9}$$

These represent four physical characteristics; the vertical direction dr = 0 is not a characteristic. This is different from the results obtained by using the stress-displacement approach, where in addition to these four characteristics, the direction dr = 0 is also a physical characteristic, as shown in Appendix A. Although dr = 0 is a degenerated characteristic associated with static discontinuities, the characteristic equation along dr = 0 does supply the fifth equation for the five variables ϕ_t, w_t, M_r, M_θ, and Q_r. In using the system of equations (6) and (7), the condition of continuity in the displacement function ϕ supplies the additional equation required, as will be shown below. For a plate in which E, ρ, and ν are constant the two wave speeds, as given by (8) and (9), are constant and the physical characteristics are straight lines when represented in the r,t-plane.

The characteristic equations (sometimes known as the compatibility equations) along I^+ and I^- are, respectively,

$$\frac{1}{c_p} d\phi_t \mp d\phi_r = \mp\left[\frac{k_2^2 Gh}{D}\left(\phi + w_r\right) + \frac{\phi}{r^2} - \frac{\phi_r}{r}\right] dr \tag{10}$$

where the upper signs refer to I^+, the lower signs to I^-. The characteristic equations along II^+ and II^- are, respectively

$$dw_r \mp \frac{1}{k_2 c_2} dw_t = -\left[\frac{1}{r}\left(\phi + w_r\right) + \phi_r\right] dr \tag{11}$$

These four equations, (10) and (11), govern the variation of the variables w_r, w_t, ϕ_r, ϕ_t, and ϕ, along the physical characteristic directions. An additional equation based on the continuity of ϕ, or

$$d\phi = \phi_r dr + \phi_t dt \tag{12}$$

can be written along any direction. For instance, along a vertical direction $dr = 0$, (12) may be written as

$$d\phi = \phi_t dt \tag{13}$$

Along I^+ and I^-, it becomes

$$d\phi = \left(\phi_r \pm \phi_t \frac{1}{C_p}\right) dr \tag{14}$$

Or, along II^+ and II^-,

$$d\phi = \left(\phi_r \pm \phi_t \frac{1}{\rho_2 C_2}\right) dr \tag{15}$$

III. Equations Governing Discontinuities

The characteristic equations (10) and (11) are applicable for continuous fields with possible discontinuity in the second derivatives of ϕ and w along the physical characteristics. Along these directions, discontinuities in the first derivatives of ϕ and w can also exist, but these will not be governed by (10) and (11). Following a similar procedure as in [6], [7], and [8] it is shown in Appendices A and B that discontinuities across I^+ and I^- are governed by the following equations

$$\delta\phi_r = A r^{-1/2} \tag{16}$$

$$\delta\phi_t = \mp C_p A r^{-1/2} \tag{17}$$

$$\delta M_r = D A r^{-1/2} \tag{18}$$

$$\delta M_\theta = \nu D A r^{-1/2} \tag{19}$$

$$\delta w_r = \delta w_t = \delta Q_r = 0 \tag{20}$$

where, for example, δM_r designates the abrupt change or "jump" in M_r. Similarly, across II^+ and II^-, we have

$$\delta w_r = B r^{-1/2} \tag{21}$$

$$\delta w_t = \mp k_2 c_2 B r^{-1/2} \tag{22}$$

$$\delta Q_r = k_2^2 G h B r^{-1/2} \tag{23}$$

$$\delta \phi_r = \delta \phi_t = \delta M_r = \delta M_\theta = 0 \tag{24}$$

It should be noted that in deriving (16) to (24), the conditions $\delta w = \delta \phi = 0$ have been used; i.e., only continuous w and ϕ functions are being considered.

IV. Initial and Boundary Conditions

The problem treated in this report involves an infinite plate with a circular hole of radius r_o, i.e., the region $r_o \leq r < \infty$. The proper initial conditions for this problem require the specification of all the four variables ϕ_r, ϕ_t, w_r, and w_t at $t = 0$. For the case of an infinite plate under no initial loads and velocity, the initial conditions are

$$\phi_r(r,0) = \phi_t(r,0) = w_r(r,0) = w_t(r,0) = 0, r_o \leq r < \infty \tag{25}$$

At $r = r_o$, a properly posed boundary condition requires the specification of two of the four functions ϕ_r, ϕ_t, w_r, and w_t. Or alternatively, by using equations (3), (4), and (5), any two of the five functions M_r, M_θ, Q_r, ϕ_t, and w_t may be specified along $r = r_o$.

Without surface tractions, the region between $r = r_o + c_p t$ and $t = 0$ in the physical plane (r vs. $c_p t$) contains the trivial solution of vanishing derivatives of ϕ and w. Along the line $r = r_o + c_p t$ these derivatives are also zero if the boundary condition at $r = r_o$, $t = 0$, does not include discontinuities in the functions ϕ_r, ϕ_t, M_r, or M_θ. When discontinuities in these variables occur at $r = r_o$, $t = 0$, they will propagate along the line $r = r_o + c_p t$ according to (16) through (20).

When discontinuous functions of w_r, w_t, or Q_r are prescribed at $r = r_o$, $t = 0$, these discontinuities will propagate along the line $r = r_o + k_2 c_2 t$, according to (21) through (24). Within the region between the lines $r = r_o + k_2 c_2 t$ and $r = r_o + c_p t$, the derivatives of ϕ and w are in general different from zero, although they vanish on the line $r = r_o + c_p t$.

V. Numerical Procedures

In performing the numerical calculations, the physical plane is first divided into a network by the characteristic lines and the differential equations are then written in finite-difference form in terms of the values of the dependent variables at the mesh points of the network. In the present problem, there are four families of characteristic lines in the physical plane, with each characteristic intersecting the other three. The resulting network contains too many irregular mesh points to be practical for numerical calculations.

This is different from the case of propagation of dilatational waves as treated in Reference 7. In that case, the points of intersection between dr/dt = c and dr/dt = -c characteristics, were so arranged that they were always situated on the dr = 0 characteristics. In treating wave propagation in Timoshenko beams, Leonard and Budiansky [5] showed that there are also four families of characteristics, just as in the present case. However, in the numerical solution, they chose a special case where the wave propagation velocity of two of the four families was identical with the other two families, which essentially reduced it to a two characteristic family problem.

For the present problem, evenly spaced I^+ and I^- characteristics are used as the main network as shown in Fig. 1. Only properties at these mesh points will be calculated. The values of all the dependent variables w_r, w_t, ϕ_r, ϕ_t, and ϕ at a typical interior point 1 may be calculated if the corresponding values at neighboring points 2, 3, and 4 are known from previous calculations. Draw II^+ and II^- characteristics from point 1, which intersect the I^- and I^+ characteristics (which pass through point 4) at points 5 and 6, respectively. Values of the variables at points 5 and 6 are obtained from those at points 2, 4, and 3 by linear interpolation. The characteristic equation (10) with the upper sign is then written in finite-difference form between points 1 and 2. Similarly, along a I^- between points 3 and 1, along a II^+ between points 5 and 1, and along a II^- between points 6 and 1, the corresponding characteristic equations are also expressed in finite-difference form. These finite-difference equations are

Along I^+ :

$$\frac{1}{c_p}\left[\phi_{t_1}-\phi_{t_2}\right]-\left[\phi_{r_1}-\phi_{r_2}\right]=-\frac{k_2^2 G h}{D}(r_1-r_2)\left\{\phi_{12}+w_{r_{12}}\right\}$$

$$-(r_1-r_2)\left\{\phi_{12}/r_{12}^2\right\}+(r_1-r_2)\left\{\phi_{r_{12}}/r_{12}\right\} \qquad (26)$$

Along I^- :

$$\frac{1}{c_p}\left[\phi_{t_1}-\phi_{t_3}\right]+\left[\phi_{r_1}-\phi_{r_3}\right]=\frac{k_2^2 G h}{D}(r_1-r_3)\left\{\phi_{13}+w_{r_{13}}\right\}$$

$$+(r_1-r_3)\left\{\phi_{13}/r_{13}^2\right\}-(r_1-r_3)\left\{\phi_{r_{13}}/r_{13}\right\} \qquad (27)$$

Along II^+ :

$$\left[w_{r_1}-w_{r_5}\right]-\frac{1}{k_2 c_2}\left[w_{t_1}-w_{t_5}\right]=-\frac{1}{r_{15}}\left\{\phi_{15}+w_{r_{15}}\right\}(r_1-r_5)$$

$$-\phi_{r_{15}}(r_1-r_5) \qquad (28)$$

Along II^- :

$$\left[w_{r_1}-w_{r_6}\right]+\frac{1}{k_2 c_2}\left[w_{t_1}-w_{t_6}\right]=-\frac{1}{r_{16}}\left\{\phi_{16}+w_{r_{16}}\right\}(r_1-r_6)$$

$$-\phi_{r_{16}}(r_1-r_6) \qquad (29)$$

In addition, the continuity condition for ϕ along dr = 0, equation (13), in difference form is used,

$$\phi_1-\phi_4=\phi_{t_{14}}(t_1-t_4) \qquad (30)$$

In these equations, (26) to (30), a numeral subscript indicates the point at which the quantity is evaluated, a double numeral subscript designates the average between the two points. These five equations, (26) to (30), can be solved for the five unknowns ϕ, ϕ_r, ϕ_t, w_r, and w_t at point 1. Notice that in writing these equations only central differencing and averaging operations have been used, and since the equations are linear, the truncation error is of the $(\Delta r)^2$ type.

For points along the line $r = r_o$, the I^+ and II^+ characteristics, represented by equations (26) and (28), are absent. Since two of the variables ϕ_r, ϕ_t, w_r, and w_t are specified along the $r = r_o$ line, the remaining three equations (27), (29), and (30) are sufficient for finding the three remaining unknowns, i.e., ϕ together with the two unspecified variables among ϕ_r, ϕ_t, w_r, and w_t . If M_r and Q_r are specified along $r = r_o$, then eqs. (3) and (5) will replace eqs. (26) and (28) and the system of five governing equations necessary for the determination of the five variables is again complete.

VI. Approximate "Jump Line"

When the input at $r = r_o$ involves discontinuities (jumps) in Q_r, w_r, or w_t, these discontinuities propagate along the II^+ line which has an equation $r = r_o + \mu t'$, where $\mu = k_2 c_2/c_p$ and $t' = c_p t$. This line, in general, does not intersect the main network at the mesh points, as shown in Fig. 2. One way of treating this line is to introduce a new irregular mesh point wherever this line intersects the main network. This would introduce a considerable amount of complexity and therefore, is not being used here. Instead, the straight line

$r = r_o + \mu t'$ will be replaced by a line passing through regular mesh points, but with a discontinuous slope. This line will be called the approximate jump line or simply, jump line. The construction of this line and the procedure in treating the jumps across it will be given below.

Let us introduce a new coordinate system (α,β) which consists of the I^+ and I^- characteristics as shown in Fig. 2. The finite-difference network is then composed of constant α and constant β lines, with constant increment $\Delta\alpha = \Delta\beta$. The point of intersection between the line $r = r_o + \mu t'$ and a particular α = constant line, say $\alpha = m(\Delta\alpha)$ line, where m is an integer, is at

$$\beta = \left(\frac{1-\mu}{1+\mu}\right) m(\Delta\alpha) \tag{31}$$

In general, this β is not an integer and therefore is not located at a regular mesh point. In constructing the jump line, this point will be moved to the nearest regular mesh point along the $\alpha = m(\Delta\alpha)$ line. This is achieved by letting

$$\beta = \left(\frac{1-\mu}{1+\mu}\right) m(\Delta\alpha) = (n+\epsilon)\,\Delta\alpha \tag{32}$$

where n is an integer and $0 \leq \epsilon < 1$. For a particular value of m, if $\epsilon < 0.5$, the jump point is moved to $\alpha = m(\Delta\alpha)$, $\beta = n(\Delta\alpha)$; if $\epsilon \geq 0.5$, it is placed at $\alpha = m(\Delta\alpha)$, $\beta = (n+1)(\Delta\alpha)$. The jump line is then drawn by connecting these points with straight line segments of constant β or constant r, shown in Fig. 2(a) as a heavy "zig-zag" line. It is evident that as the mesh size $\Delta\alpha$ approaches zero, the jump line approaches the straight line $r = r_o + \mu t'$ as a limit.

At the mesh points on the jump line, each of the variables w_r, w_t, and Q_r assumes two values, e.g., w_r (unjumped value) and $w_r + \delta w_r$

(jumped value), etc., where δw_r, δw_t, and δQ_r are calculated from (21) to (23). The unjumped values of these variables should be used in these finite-difference equations which connect the points on the jump line with points to the right of the jump line; the jumped values of the variables on the jump line should be used for those equations connecting points to the left of the jump line.

Unjumped values at points such as A and B, which are not situated at the upper end of the vertical line segments of the jump line, may be calculated by the regular set of finite-difference equations (26) to (30).

Values of all variables at point F are calculated by the same set of equations, with the jumped values at points A and B. To calculate the values at points which lie at the upper end of the vertical line segments, such as point G, a different calculation procedure is employed. In the finite difference equations (26) and (28) written along the I^+ and II^+ waves (passing through point G) we must use the jumped values at point B and the jumped expressions of the variables at point G, i.e., $w_{tG} + \delta w_{tG}$, etc. In writing (27) and (29) for point G, the unjumped values at B and the unjumped expressions at G must be used. In using (30) for point G, no special procedure is required since this equation does not contain any variables with values which jump when crossing II^+. Thus, for point G, we have again five equations for the five unknowns w_{tG}, w_{rG}, ϕ_{tG} ϕ_{rG}, and ϕ_G.

An alternate procedure for approximating the $r = r_o + \mu t'$ line is as follows. The approximate jump line is constructed by straight constant α and constant β line segments, as shown by the heavy line in Fig. 2(b). At points such as A', the unjumped values of the variables are calculated first; whereas at points such as C' the jumped values are calculated from the five finite difference equations. To calculate the unjumped values

at B', the amount $\delta w_{rC'}$ and $\delta w_{tC'}$ must be subtracted from the previously calculated jumped values at C', before substituting them into the finite difference equations.

VII. Specific Examples

A few examples with different inputs at $r = r_o$ are presented below. These include inputs of ramp Q_r, ramp M_r, and step Q_r. Unfortunately, there are no solutions by any other methods which can be used to compare our results. Whenever possible, we shall calculate the long time asymptotic solution and compare it with the corresponding static solution. In [3], the case of a plate without a central hole is solved. In the hope of making some comparison with [3], a plate with a very small hole is chosen for our calculation. Unless otherwise specified, the plate dimensions and elastic properties used for all examples are as follows:

$r_o = 0.025$ in $\qquad E = 28 \times 10^6$ psi

$h = 0.125$ in $\qquad \nu = 0.3$

$\rho = 7.41 \times 10^{-4}$ lb-sec^2/in $\qquad k_2^2 = 0.85$

$\Delta r = 0.0125$ in

The calculated plate velocity c_p is 2.03774×10^5 in/sec., and shear velocity $k_2 c_2$ is 1.11146×10^5 in/sec. The value for the shear correction factor k_2^2 should be between 0.76 and 0.91, [2]. Since the value of 0.85 was used in [3], the same value is used here for comparison purposes.

The calculations were performed on an IBM 7040 computer, with an average running time of 20 minutes for each example.

A. Ramp Q_r Input

The first example is that of a plate under ramp Q_r and zero M_r input at $r = r_o$, for which the proper boundary conditions are

at $r = r_o$, $t > 0$, $M_r = 0$

$Q_r = (1/k)t$ lb/in for $t < k$

$= 1$ lb/in for $t > k$

where $k = 1.227$ μsec. is used.

The response of the plate due to this input is shown in Fig. 3. Fig. 3(a) shows the shear force Q_r plotted as a function of time, at three different radii. On the curve for $r/h = 1$, four points are marked and labeled 1, 2, 3, and 4. Points 1 and 2 correspond to the time of arrival of the I^+ and II^+ waves, respectively, from $r = r_o$, $t = 0$. Points 3 and 4 are at the time of arrival of the I^+ and II^+ waves from $r = r_o$, $t = k$, i.e., the point of discontinuous dQ_{ro}/dt in the input. The change in slope of Q_r is barely discernible at point 4. As the wave propagates outwards this discontinuity in slope diminishes and cannot be noticed at $r/h = 2$ or $r/h = 3$. At $r/h = 1$, the Q_r curve first goes downwards, then increases to a peak value, and eventually settles to an asymptotic value at large time. From the static equilibrium of the portion of the plate bounded by r_o and an arbitrary r, we have

$$2\pi r_o Q_{ro} = 2\pi r Q_r$$

or

$$Q_r = \frac{r_o}{r}$$

for $Q_{ro} = 1$. At $r/h = 1$, or $r = 0.125$ in., the static Q_r is 0.20. The calculated asymptotic value of Q_r approaches this static value at large time, as can be seen from Fig. 3(a). At $r/h = 2$ and $r/h = 3$ there are no peak values for Q_r, although the long time values also approach those of the static solution.

In Figs. 3(b) and 3(c), the moments M_r and M_θ are given as function

of time, at the three radii. As expected, at large times the absolute values of the moments increase monotonically. The maximum moment in the plate is M_θ which occurs at the hole, $r = r_o$. This moment, as a function of time, is plotted separately in Fig. 3(d).

Calculation of this problem with a mesh size one-half of the one used above gives essentially the same numerical results. This indicates that the accuracy by using the present mesh size ($\Delta r = 0.0125$ in.) is satisfactory.

B. Ramp M_r Input

The radius of the hole for this case is taken as $r_o = 0.25$ in. The proper boundary conditions used are

at $r = r_o$, $t > 0$

$$Q_r = 0$$

$$M_r = (1/k)\ t \text{ in-lb/in} \quad \text{for } t < k$$

$$= 1 \text{ in-lb/in} \quad \text{for } t \geq k$$

($k = 1.227$ μsec.)

For a plate of this geometry under a static load M_{ro} at $r = r_o$, it can be shown that the static solutions are, [9].

$$Q_r = 0$$

$$M_r = -M_\theta = \left(\frac{r_o}{r}\right)^2 M_{ro}$$

Our calculated results are presented in Fig. 4. Fig. 4(a) gives the M_r vs. t curves, 4(b) gives the M_θ vs. t curves and 4(c) gives the Q_r vs. t curves, all evaluated at three different radii. All curves approach their corresponding static values at large time. The moments and shear attenuate very slowly, for instance, at a time of 30 μsec. all values are still slightly different from their static values.

C. Step Q_r Input

Due to the approximation involved in replacing the line $r = r_o + \mu t'$ by the jump line, the accuracy in the case of the step Q_r input is not as good as those of the ramp inputs, where the jump line approximation is not used. Therefore, a smaller mesh size, $\Delta r = 0.00625$ in. was used. The boundary conditions are

at $r = r_o$, $M_r = 0$

$Q_r = 0$ for $t = 0$

$= 1$ lb/in for $t > 0$

Because of the small hole size ($r_o/h = 0.2$), the response of the plate should be very close to that of a plate without a hole. Strictly speaking, a zero slope boundary condition ($\phi = 0$ at $r = r_o$) with r_o shrinking to zero represents more closely a plate without a hole. However, our calculations indicate that the results of $M_r = 0$ and that of $\phi = 0$ are almost identical in regions not too close to the hole. Comparing our Fig. 5 with Figs. 3, 4, and 5 of [3] it can be seen that our Q_r, M_r, and M_θ curves are in general agreement with those calculated by Miklowitz for a plate without a hole.

A slight difference exists, however, between our results and those of [3]. According to [3], the magnitude of δQ_r, the discontinuity in Q_r across the II^+ wave front, is infinity. Our equation (23) indicates that δQ_r decreases as the wave propagates outward and is proportional to $1/r^{1/2}$. If the applied concentrated shear load is finite, and if this shear load is distributed over a circle of small but finite radius, r_o, such that Q_{ro} is finite, then, Q_r will always be finite and will decrease in magnitude as it propagates outwards. The propagation of an infinite δQ_r in [3] is due to the fact that a

finite shear force, Q , is being treated as an infinite shear per unit length, Q_r, at r = 0, as shown below. For a suddenly applied (step) shear force of constant magnitude, we have

$$Q = 2\pi r_o Q_{r_o} = 2\pi r_o \delta Q_{r_o}$$

According to equation (23), then

$$\delta Q_r = \delta Q_{r_o}\sqrt{\frac{r_o}{r}} = \frac{Q}{2\pi\sqrt{r_o r}}$$

As r_o approaches zero, the limit value for δQ_r is $\delta Q_r = \lim_{r_o \to 0} \frac{Q}{2\pi\sqrt{r_o r}} \longrightarrow \infty$

The accuracy of the calculation for this case is not to our satisfaction. The long time asymptotic value of Q_r at r/h = 1 is 0.225, instead of the static value of 0.2, as shown in Fig. 5(a). The calculated data for M_r and M_θ have considerable oscillation at large time. In Figs. 5(b) and 5(c), for t > 2μsec., the average values are plotted in solid lines and the dotted lines indicate the range of scatter of the data. The data presented in Fig. 5 were calculated by the alternate procedure which approximates the II^+ line by the heavy line in Fig. 2(b). To improve the accuracy, mesh sizes smaller than 0.00625 in. are currently being employed. In addition, the procedure using the jump line shown in Fig. 2(a) is also being programmed on the computer.

D. Ramp Q_r Inputs with Different Slopes

Three ramp Q_r inputs with successively steeper ramp slopes are calculated and the results compared with those due to the step Q_r input. The curves for r/h = 1 in Fig. 3 for a ramp input with k = 1.227 μsec., and the curves in Fig. 5 for a step input are replotted in Fig. 6. In addition, the curves for Q_r, M_r, and M_θ due to ramp inputs with

$k = 0.613$ and $k = 0.307$ are also included in Fig. 6. These results show that the response of a plate due to ramp Q_r inputs with successively steeper slope approaches that due to the step Q_r input.

The fact that the response due to a step input can be approximated by that due to a steep ramp input, and vice versa, is very helpful. A true step input cannot be realized in practical cases, i.e., all loads must rise with finite time. Usually, as in the case shown in Fig. 6, the response due to a step input is more severe than that due to ramp. Therefore, the stresses and moments due to a step input may be used as the upper bounds for those due to actual loadings. Comparing the responses due to step and steep ramp inputs; if the solution for one is difficult to obtain, the solution for the other can be used as an approximation.

VIII. REFERENCES

1. Y. S. Uflyand, "The Propagation of Waves in the Transverse Vibrations of Bars and Plates," Prikl. Mat. Meh., 12, 1948, pp. 287-300 (Russian).

2. R. D. Mindlin, "Influence of Rotatory Inertia and Shear on Flexural Motions of Isotropic, Elastic Plates," Jour. of Appl. Mech., 18, 1, 1951, pp. 31-38.

3. J. Miklowitz, "Flexural Stress Waves in an Infinite Elastic Plate Due to a Suddenly Applied Concentrated Transverse Load," Jour. of Appl. Mech., December 1960, pp. 681-689.

4. J. L. Lubkin, "Propagation of Elastic Impact Stresses," ONR Progress Report No. 5, Contract No. Nonr-704(00), April 1954.

5. R. W. Leonard and B. Budiansky, "On Traveling Waves in Beams," NACA TR 1173, 1954.

6. W. E. Jahsman, "Propagation of Abrupt Circular Wave Fronts in Elastic Sheets and Plates," Proc. of the 3rd Nat. Congress of Applied Mech., 1958, pp. 115-202.

7. P. C. Chou and H. A. Koenig, "Propagation of Cylindrical and Spherical Elastic Waves by Method of Characteristics," NASA TN D-2644, February 1965.

8. J. S. Hadamard,"Lecons sur la Propagation des Ondes et les Equations de L'hydrodynamique"(Chelsea, New York, 1949), pp. 81-85.

9. S. Timoshenko and S. Woinowsky-Krieger, "Theory of Plates and Shells," McGraw-Hill Book Co., Inc., 2nd Edition, 1959, p. 58.

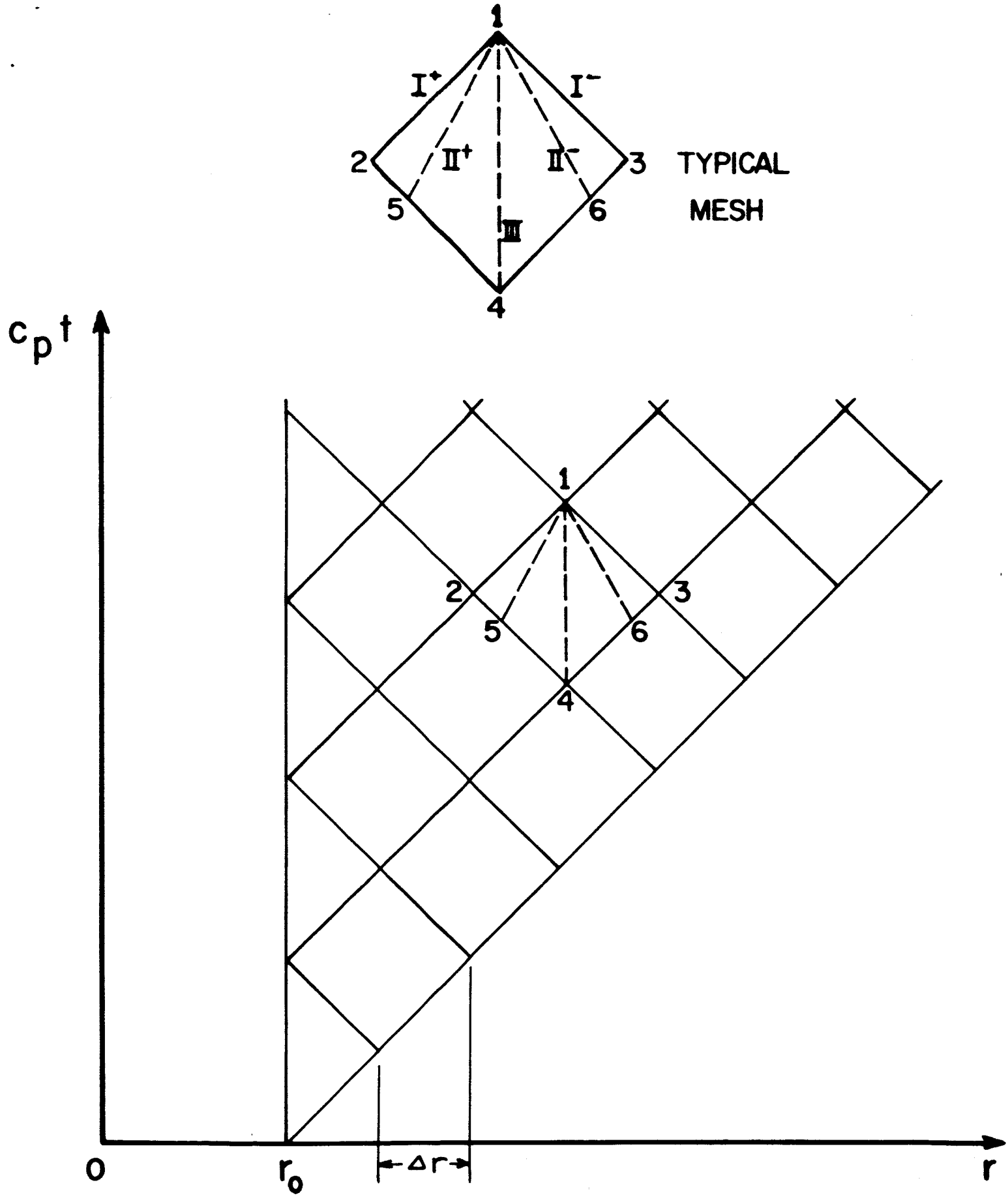

Figure 1 Characteristic Network for Application of Numerical Procedure

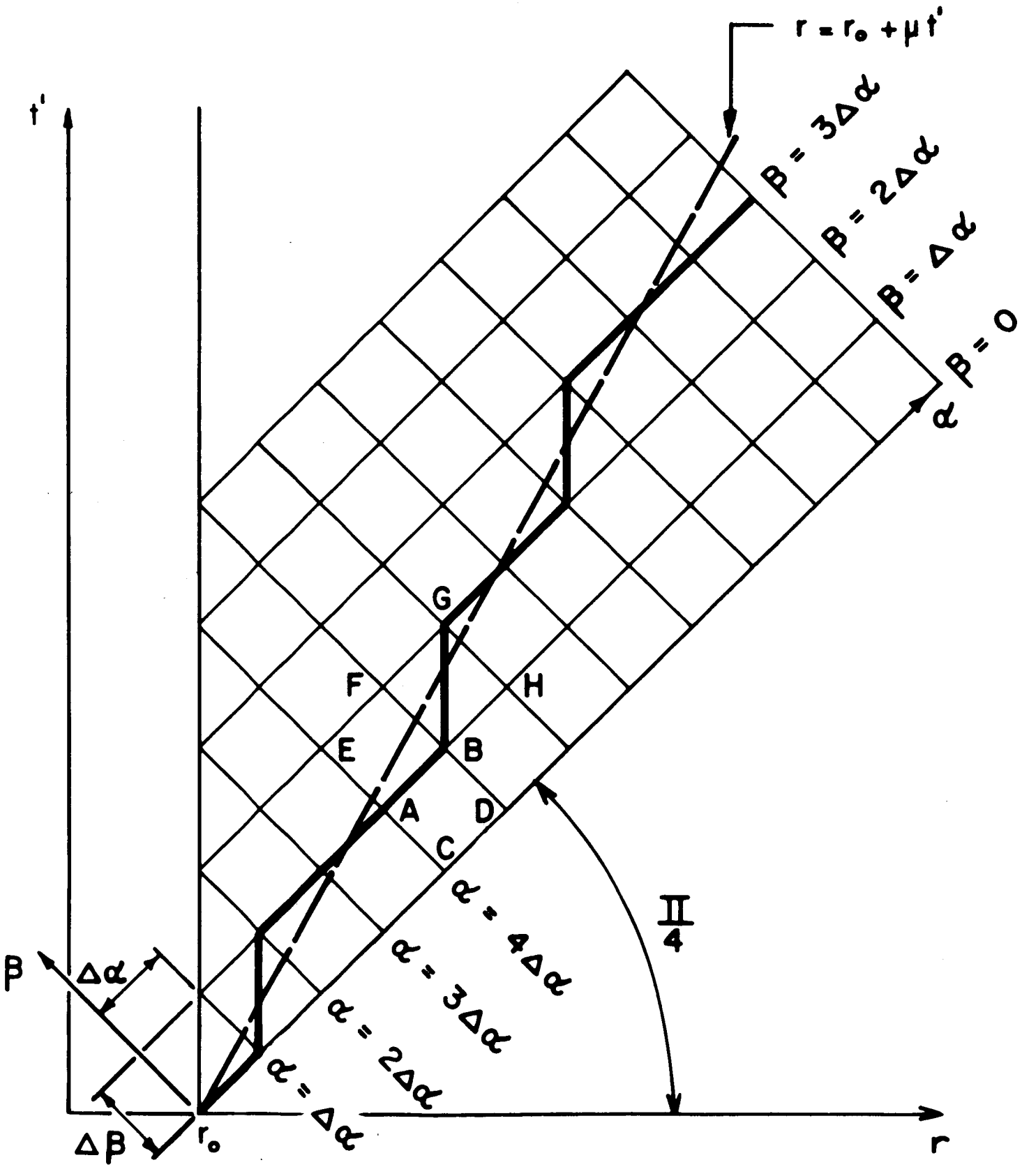

a. By straight line segments of constant β and constant r.

Figure 2. Approximations of the II^{+} Wave, $r = r_o + \mu t'$ (Jump Line)

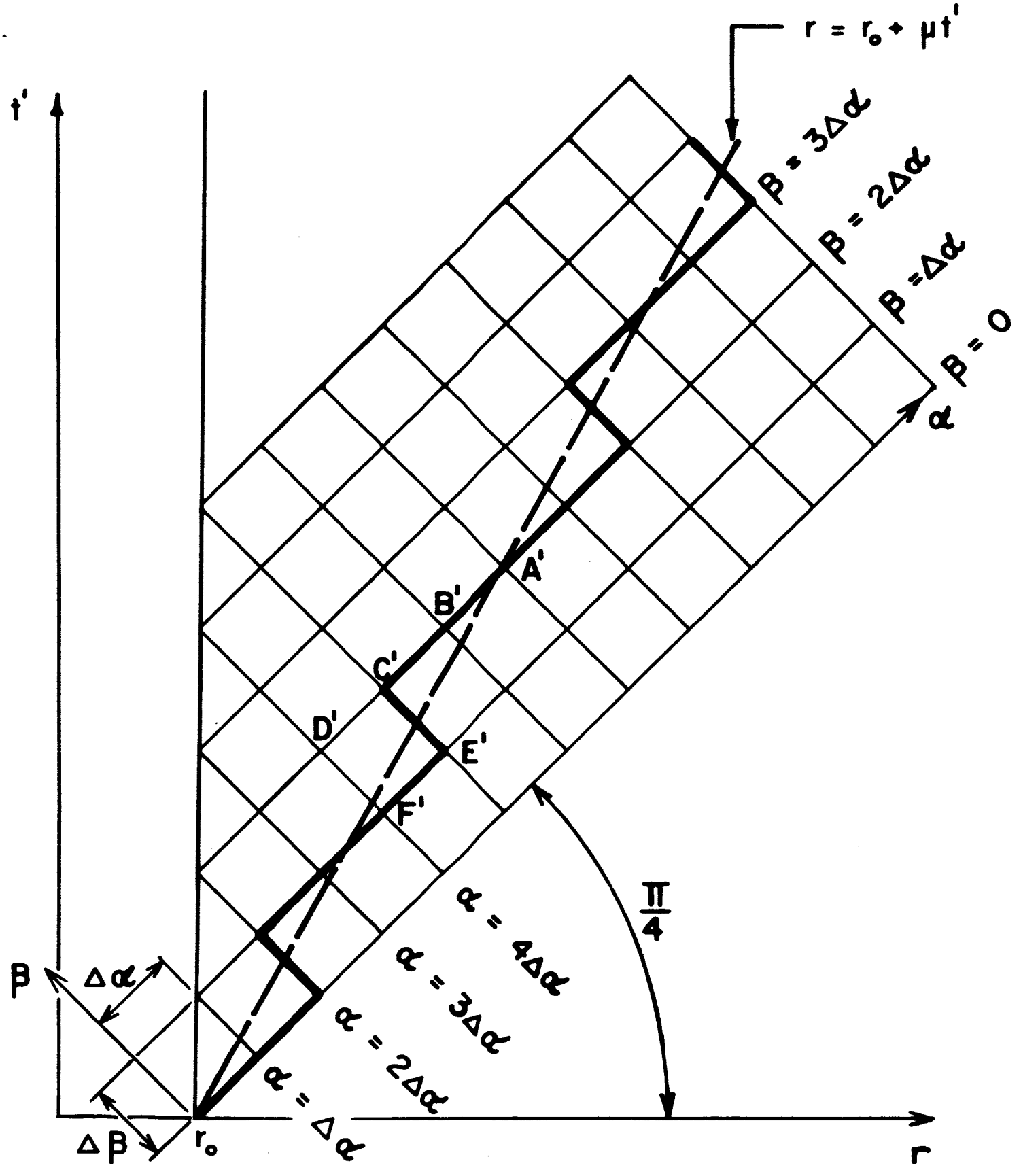

b. By straight line segments of constant β and constant α.

Figure 2. Approximations of the Π^+ Wave, $r = r_o + \mu t'$ (Jump Line)

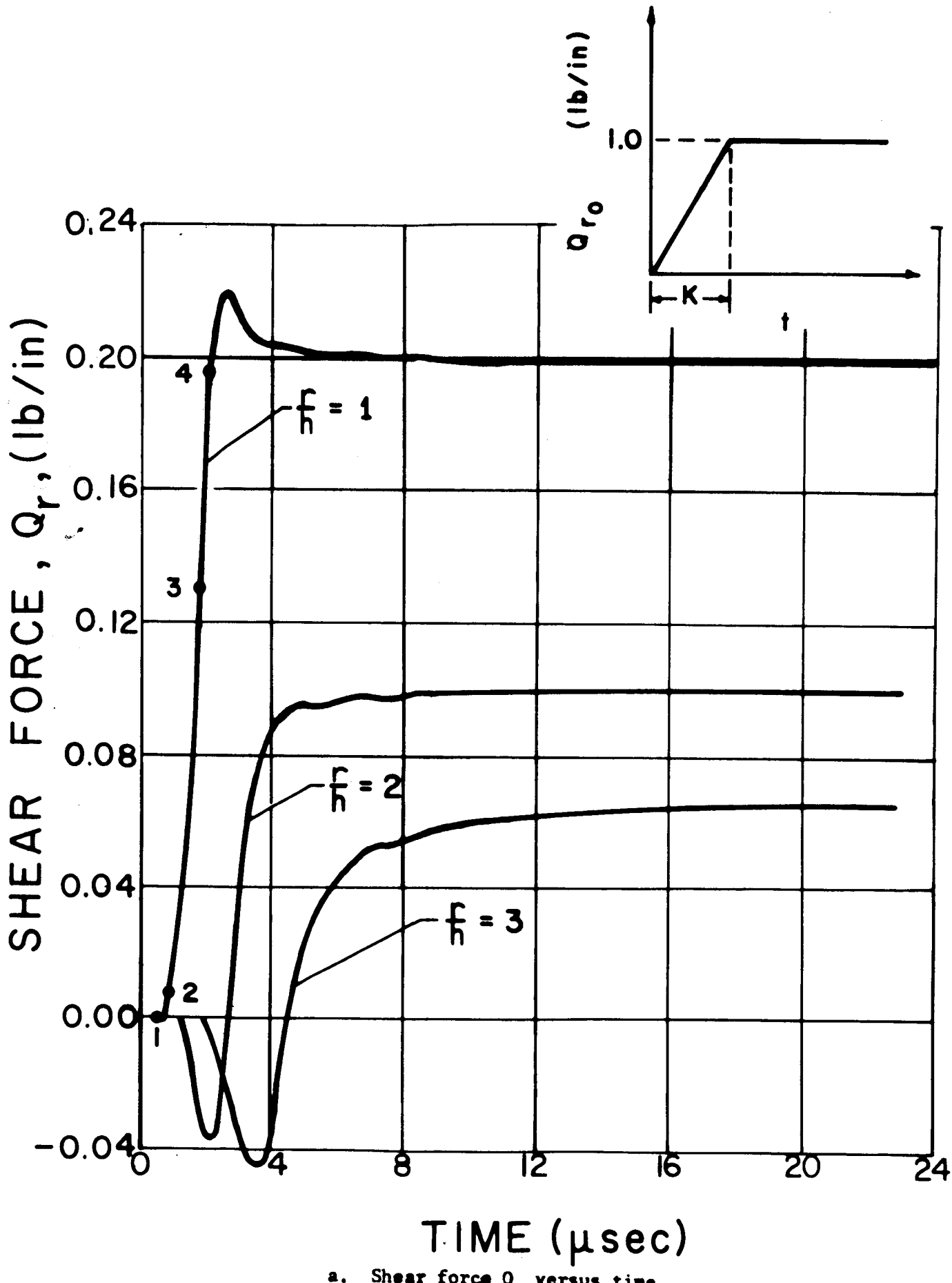

a. Shear force Q_r versus time

Figure 3 Response of a plate under a ramp Q_r input at $r = r_o$; k = 1.227μsec.

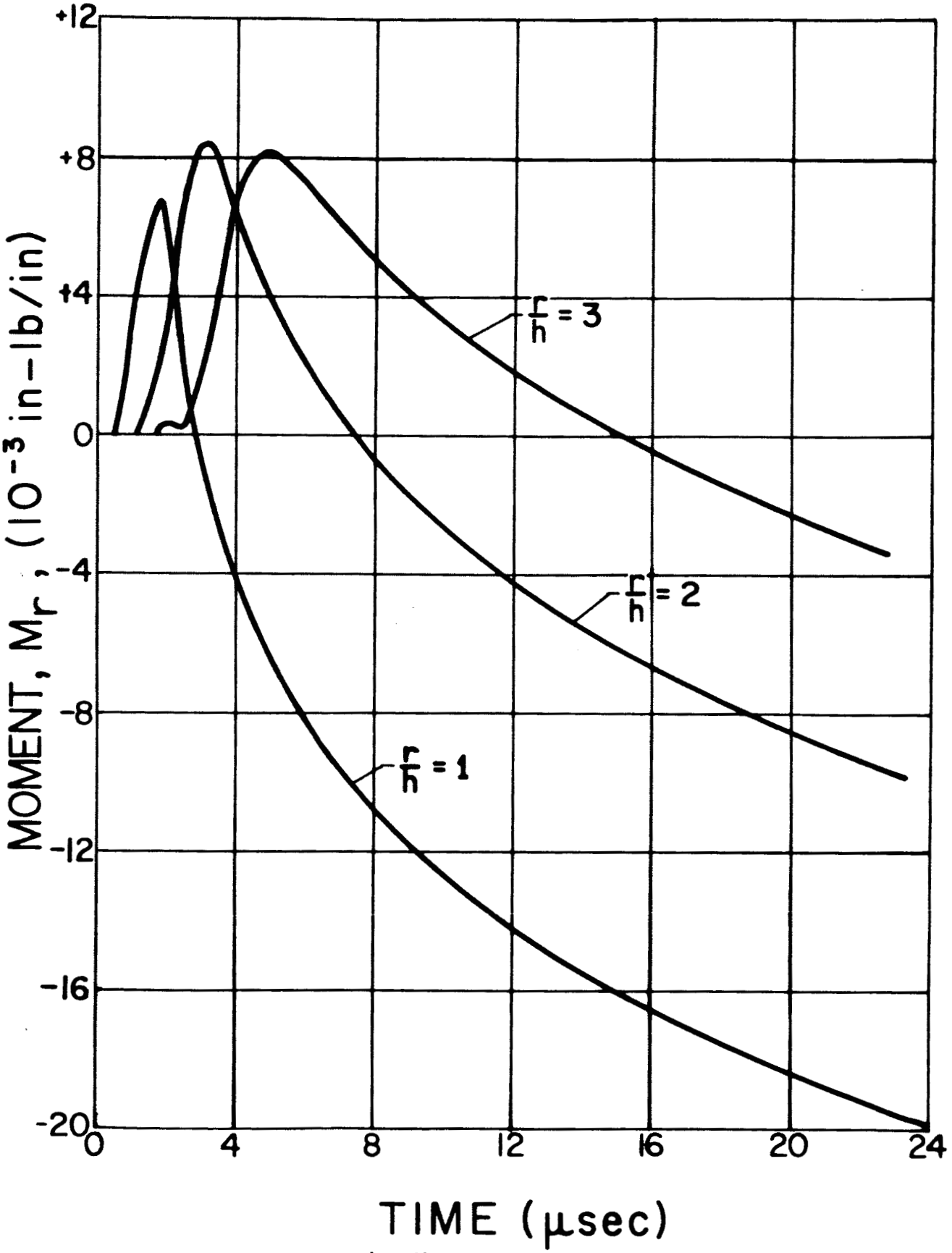

b. Moment M_r versus time.

Figure 3. Response of a plate under a ramp Q_r input at $r = r_o$; $k = 1.227\mu sec$.

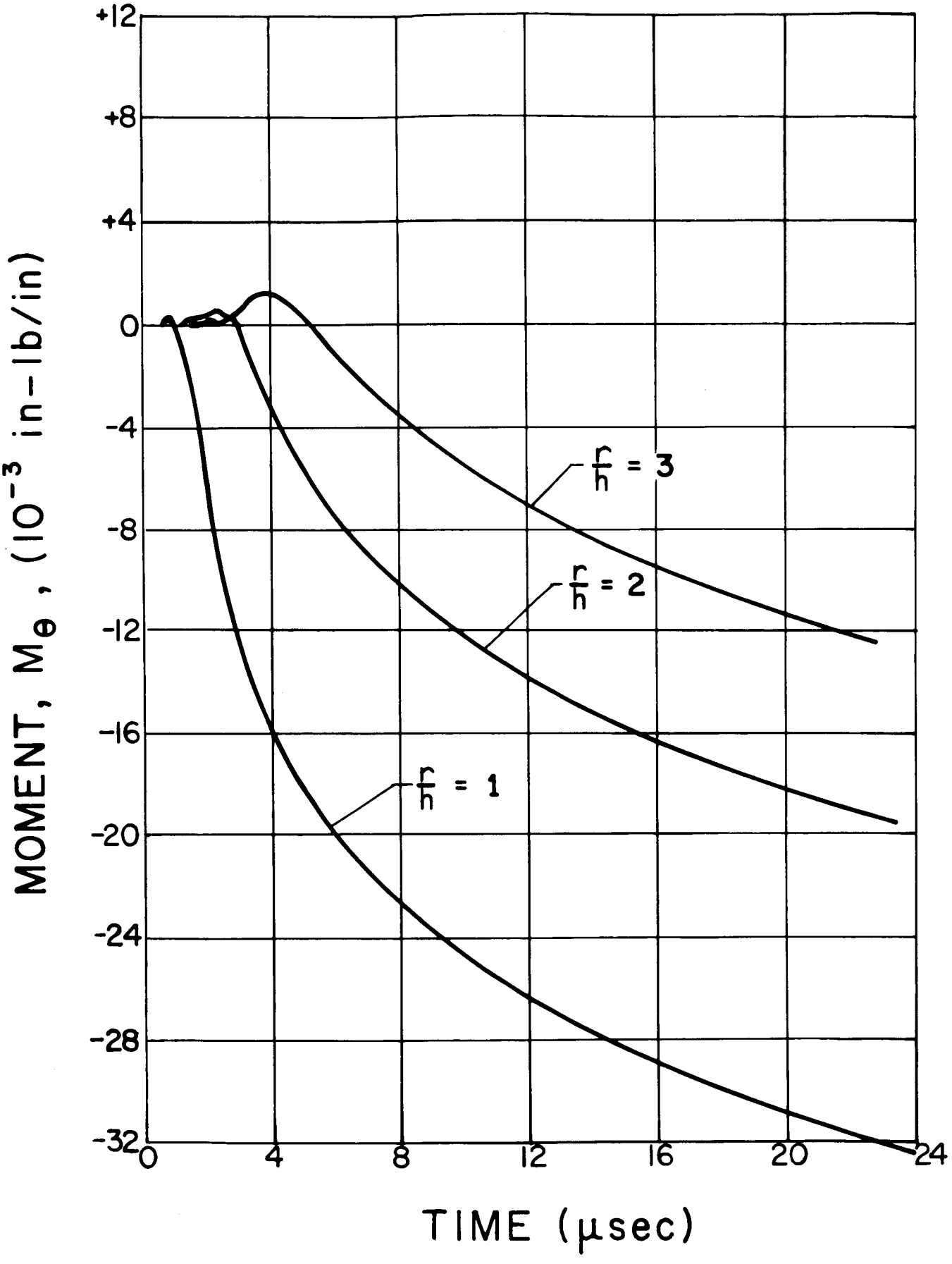

c. Moment M_θ versus time.

Figure 3. Response of a plate under a ramp Q_r input at $r = r_o$; k = 1.227μsec.

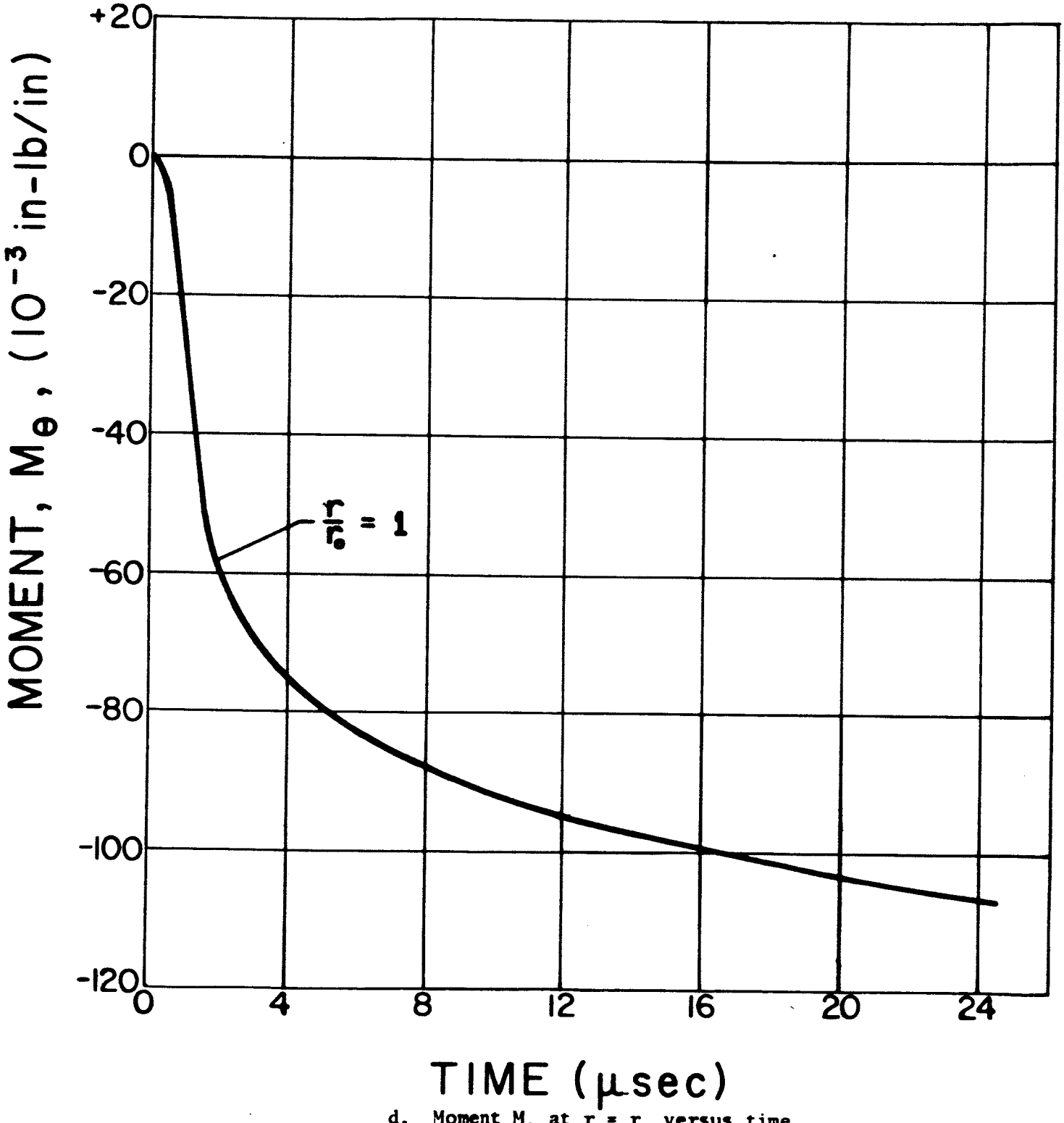

d. Moment M_θ at $r = r_o$ versus time.

Figure 3. Response of a plate under a ramp Q_r input at $r = r_o$; k = 1.227μsec.

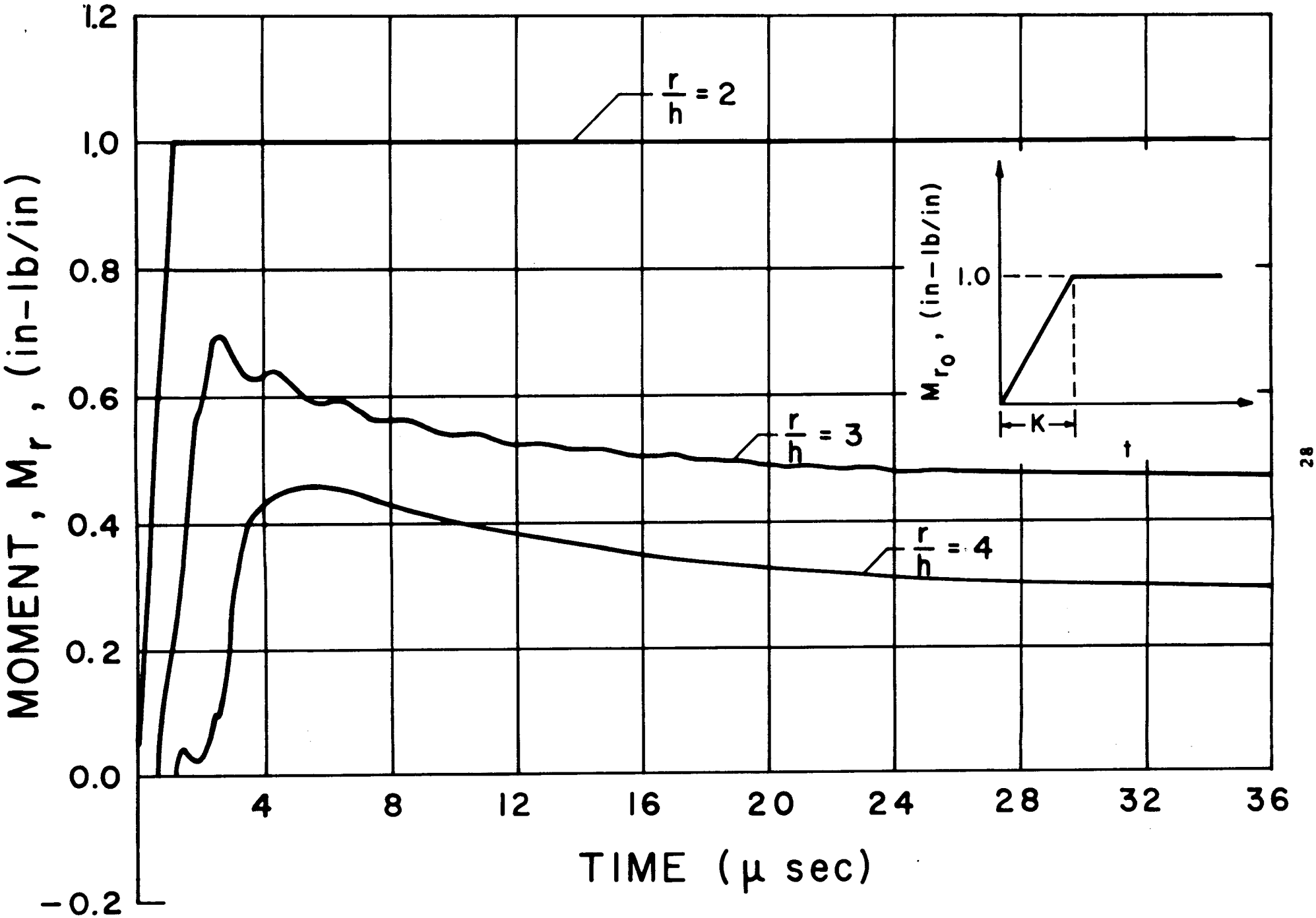

a. Moment M_r versus time.

Figure 4. Response of a Plate Under a Ramp M_r Input at $r = r_o$; k = 1.227μsec.

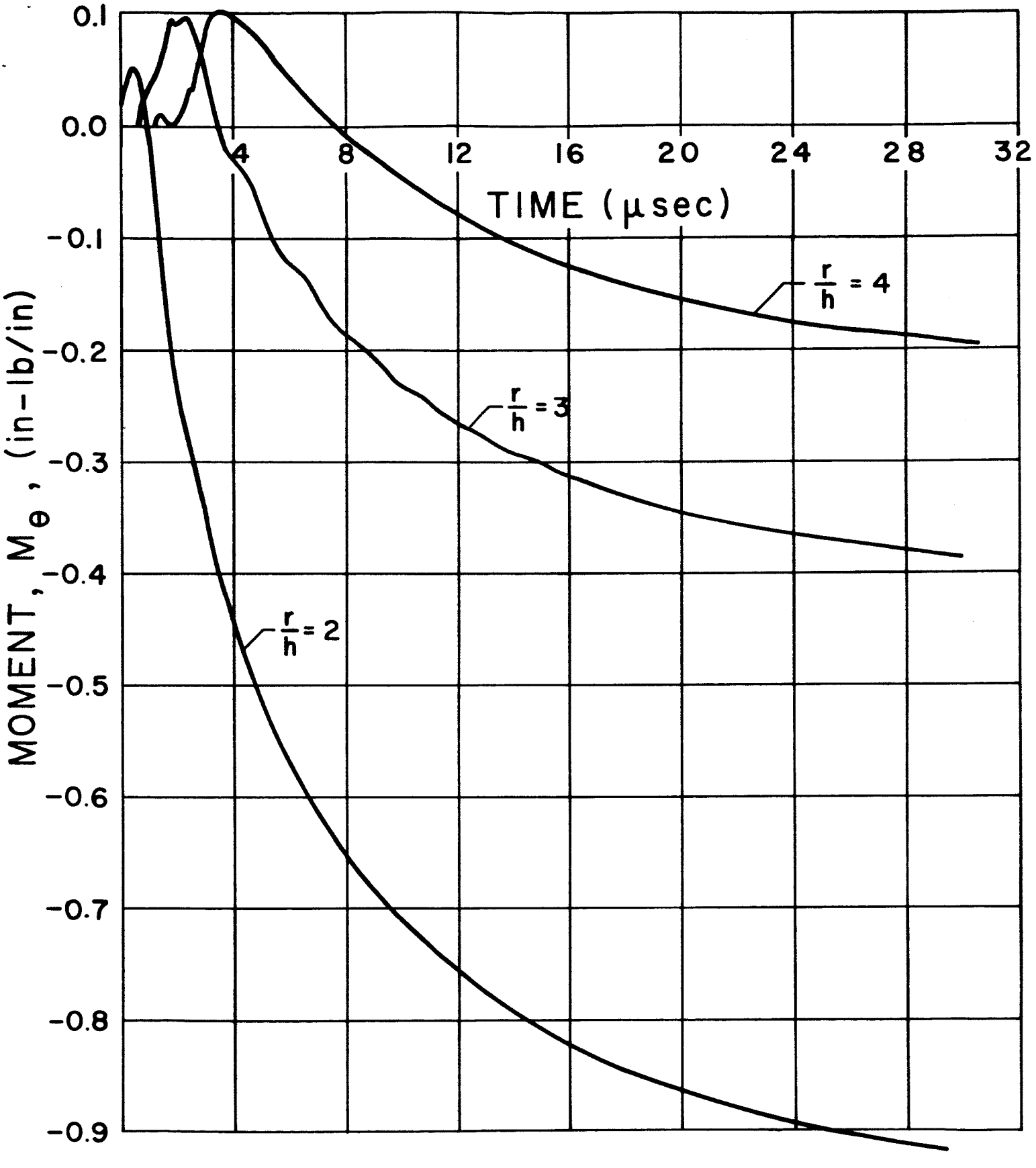

b. Moment M_θ versus time.

Figure 4. Response of a Plate Under a Ramp M_r Input at $r = r_o$; k = 1.227μsec.

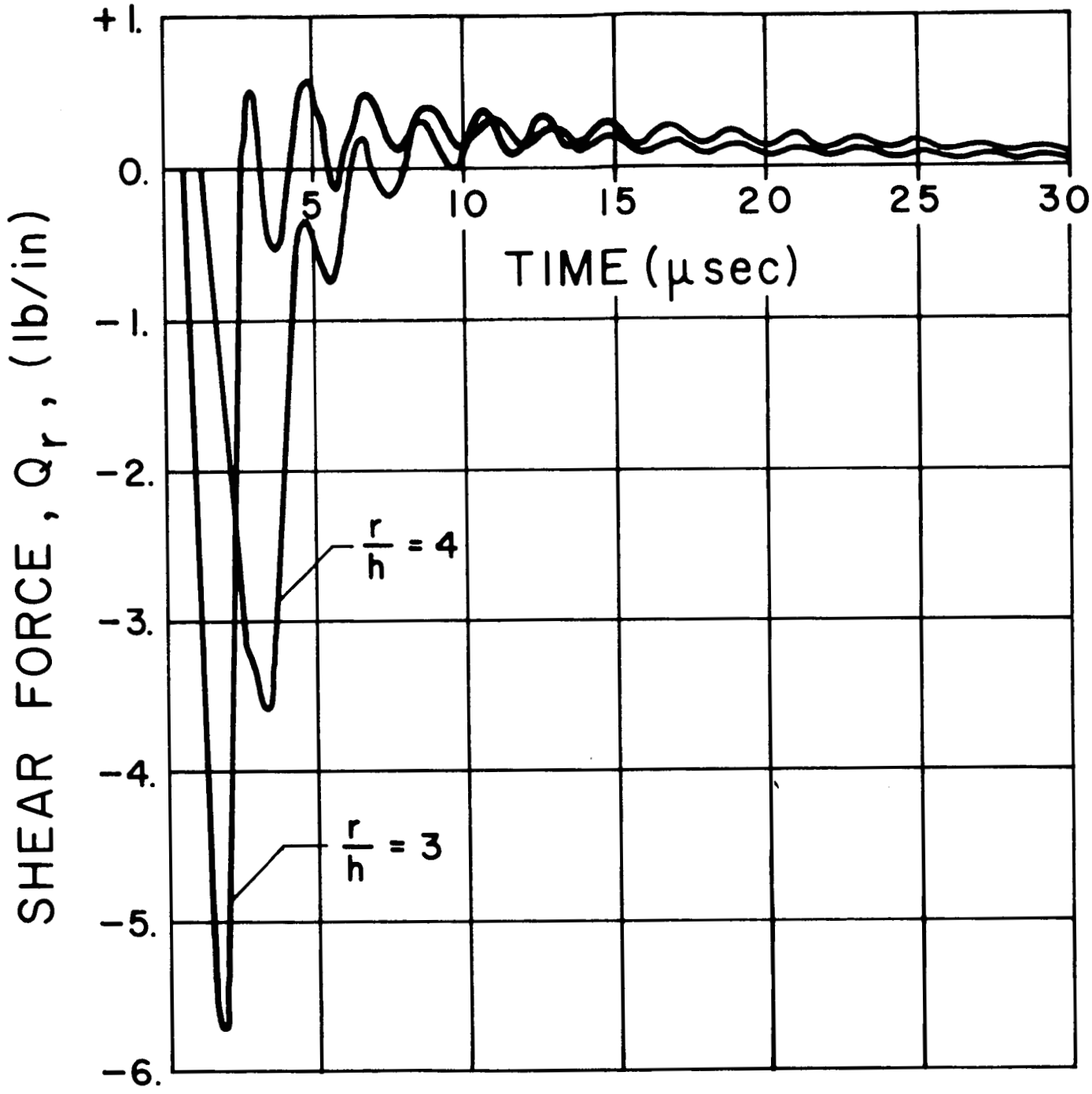

c. Shear Force Q_r versus time

Figure 4. Response of a Plate Under a Ramp M_r Input at $r = r_o$; k = 1.227μsec.

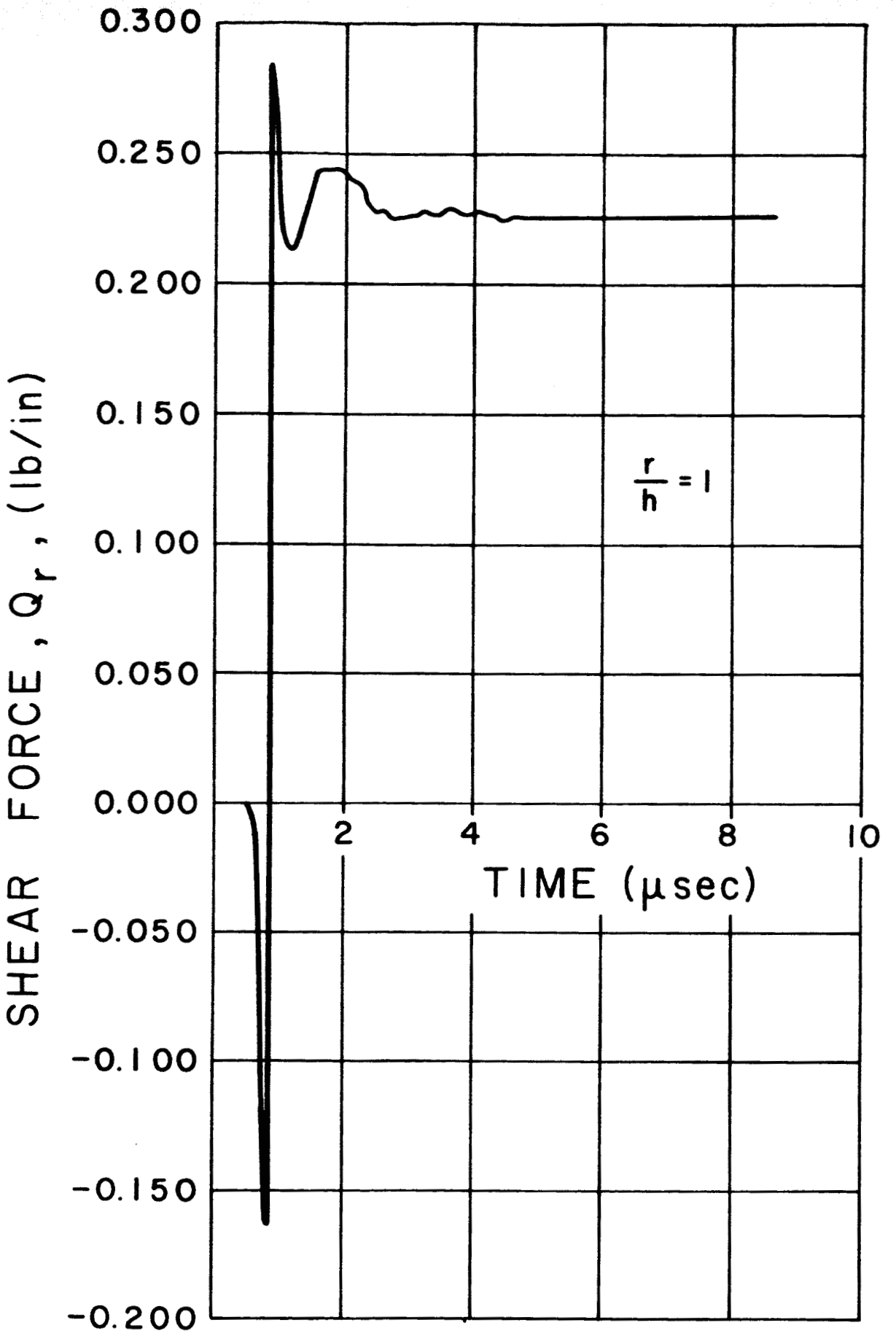

a. Shear Force Q_r versus time

Figure 5. Response of a Plate Under a Step Q_r Input at $r = r_o$

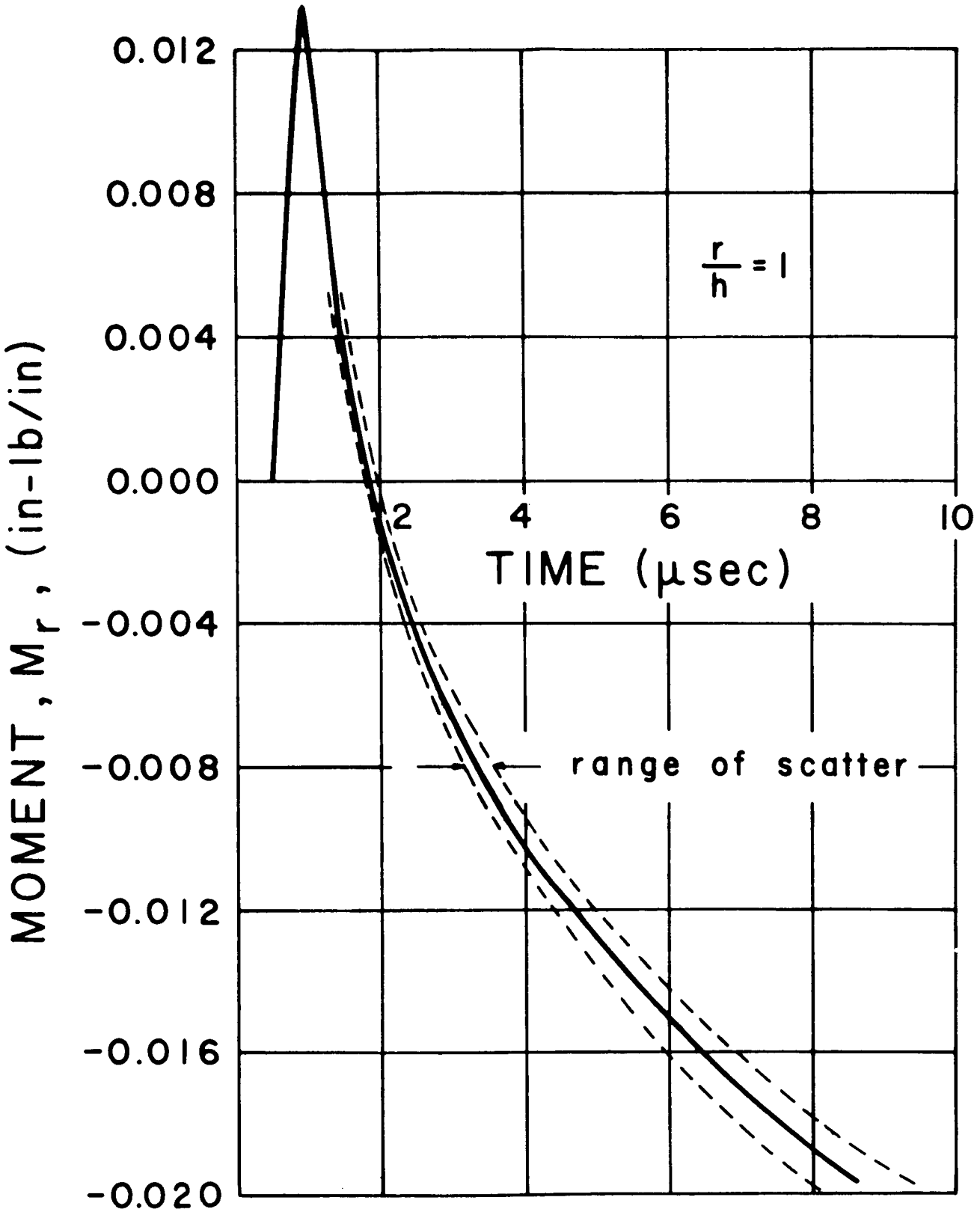

b. Moment M_r versus time.

Figure 5. Response of a Plate Under a Step Q_r Input at $r = r_o$

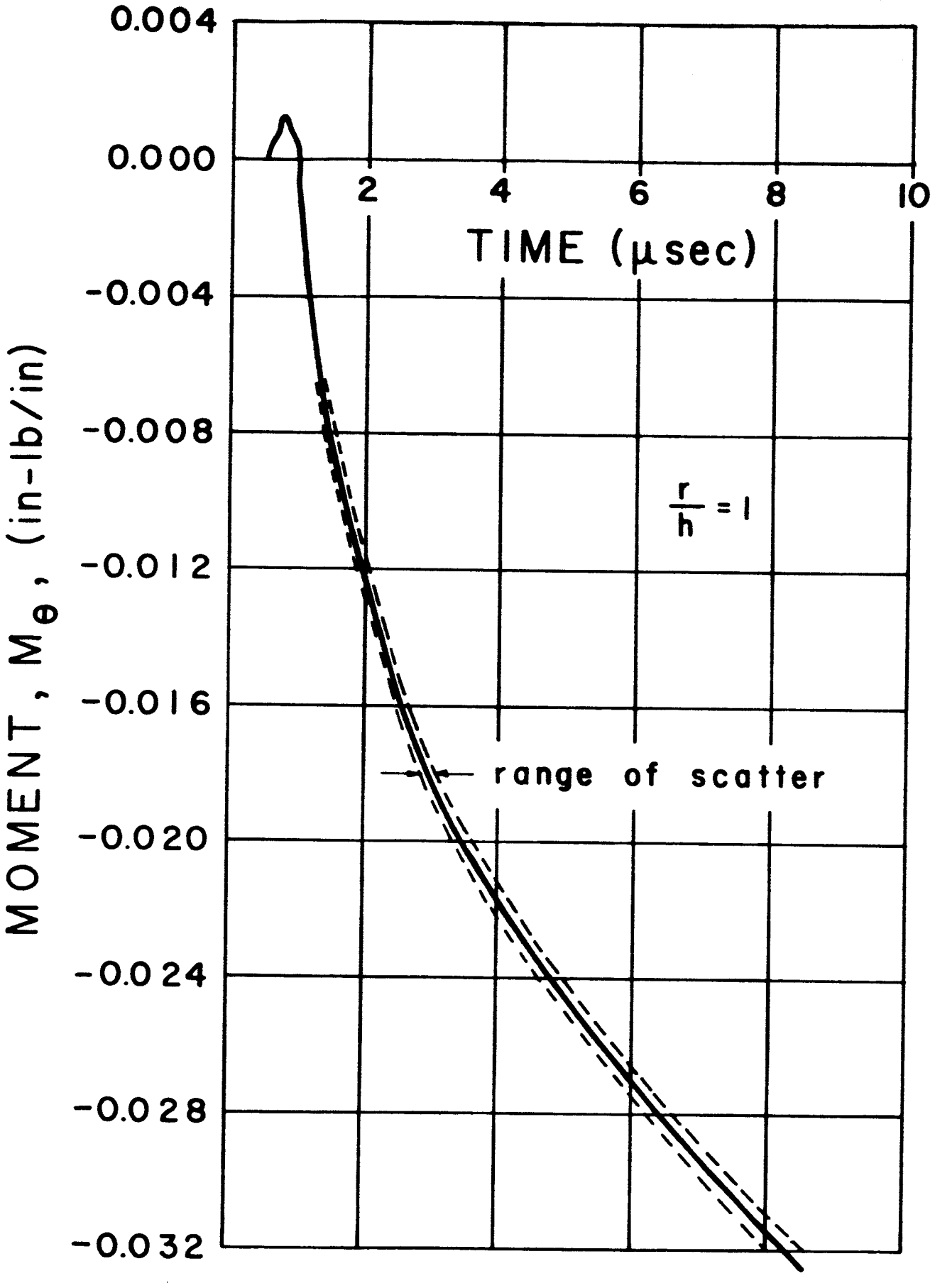

c. Moment M_θ versus time.

Figure 5. Response of a Plate Under a Step Q_r Input at $r = r_o$

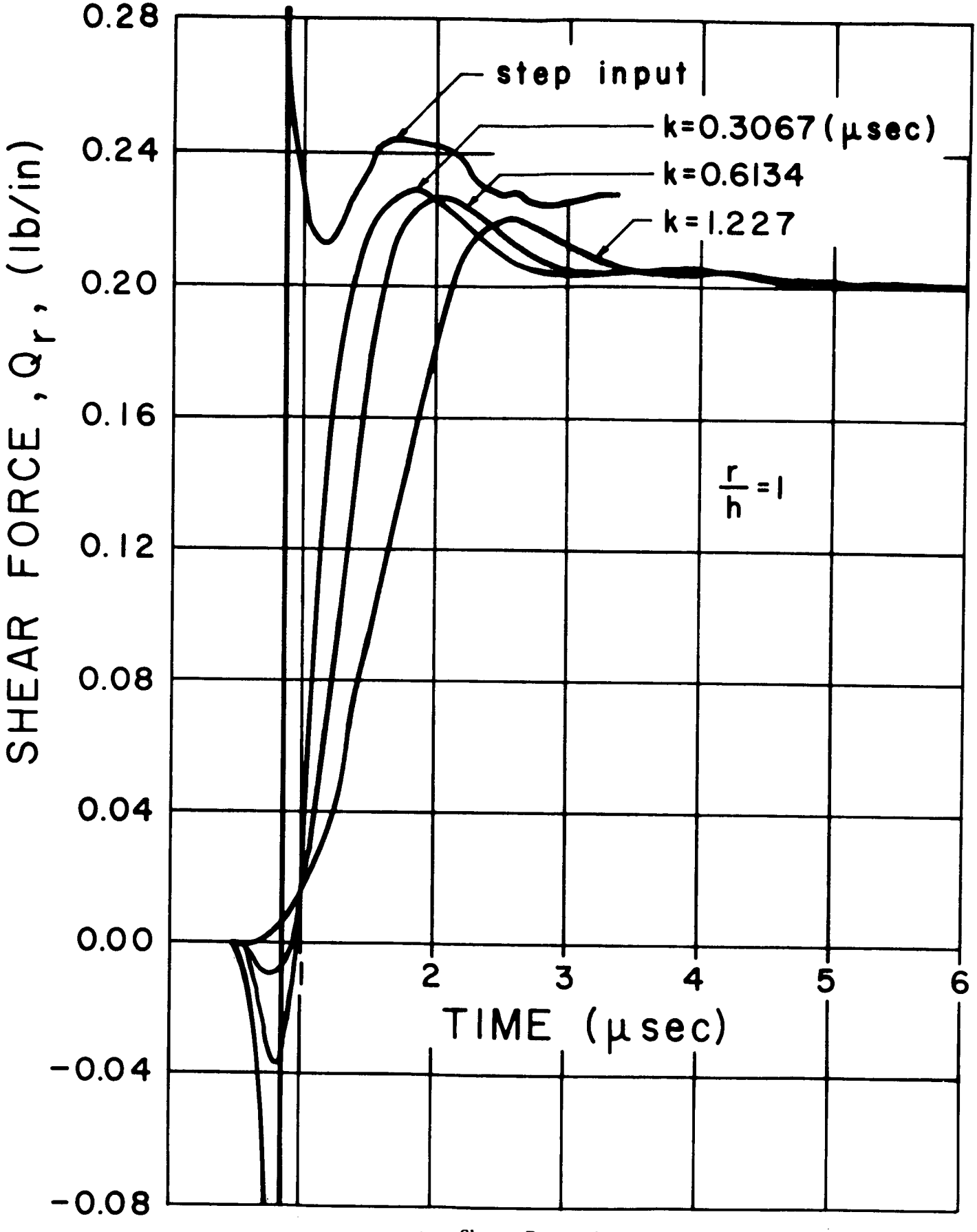

a. Shear Force Q_r versus time.

Figure 6. Results of Ramp Q_r Inputs with Different Slopes

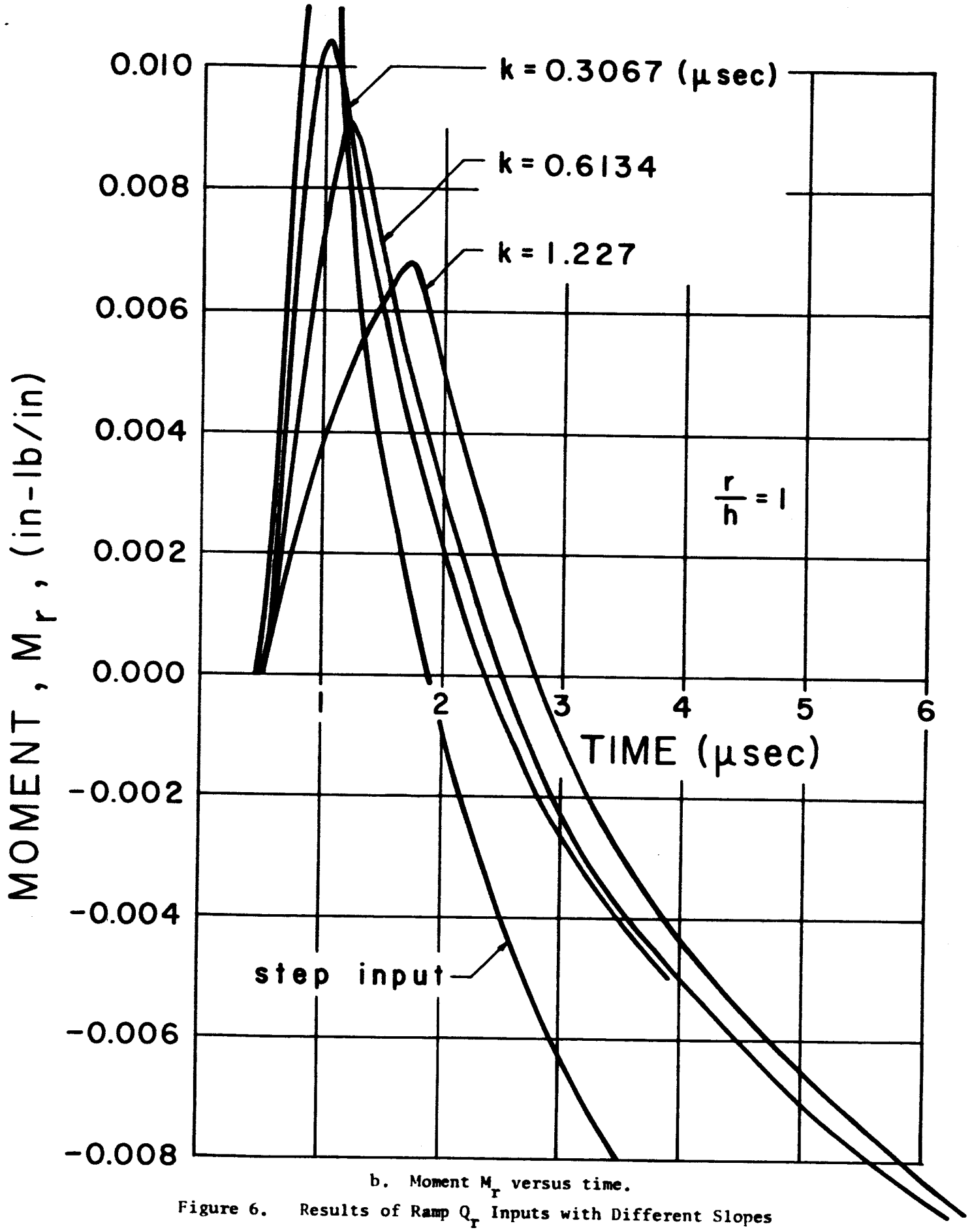

b. Moment M_r versus time.

Figure 6. Results of Ramp Q_r Inputs with Different Slopes

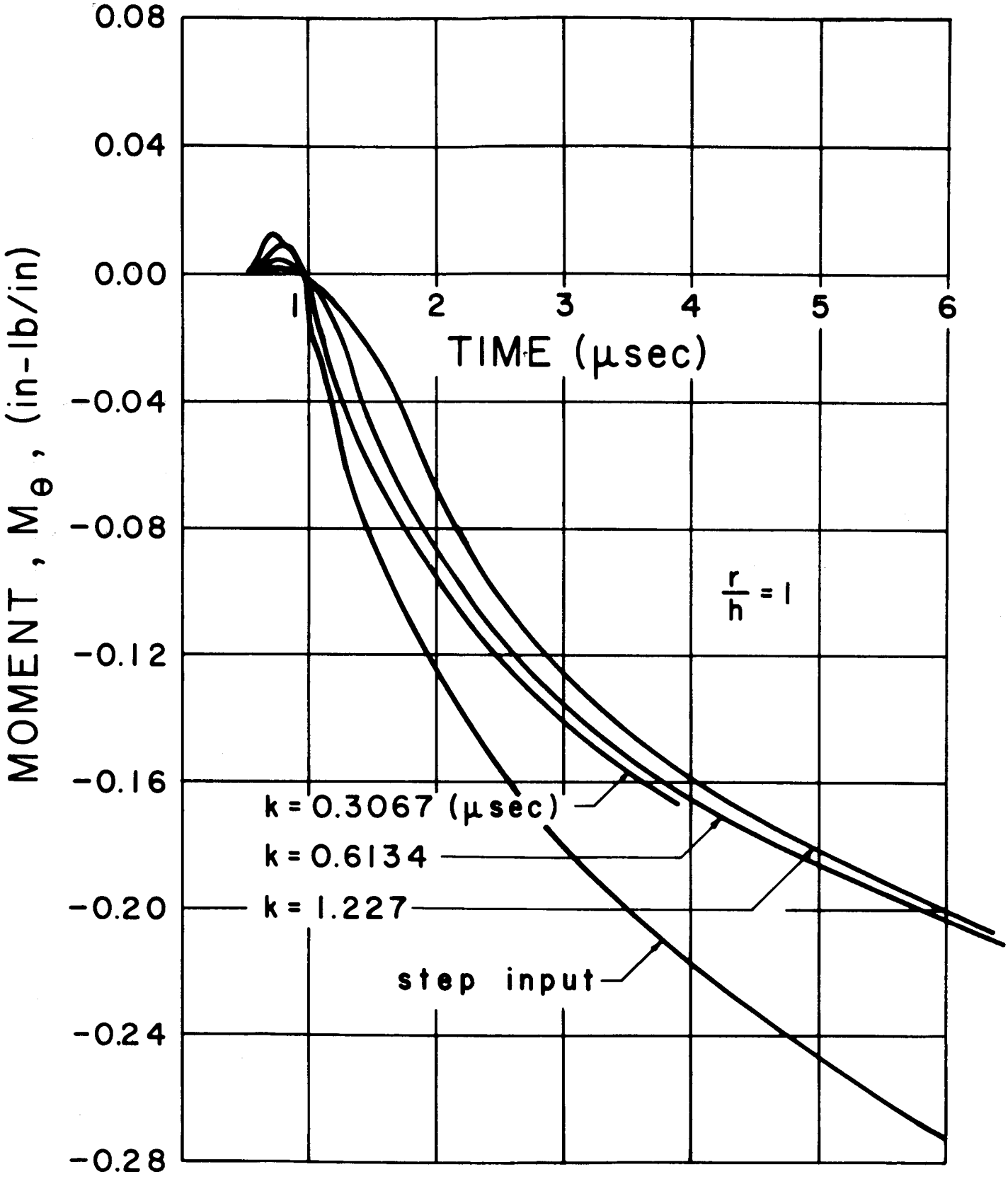

c. Moment M_θ versus time.

Figure 6. Results of Ramp Q_t Inputs with Different Slopes

APPENDIX A

Method of Characteristics - Stress Approach

Jahsman [6] has applied the method of characteristics to the stress formulation, (or more precisely, stress-displacement formulation) equations (1) to (5), of the plate problem. He used a set of plate equations with r and θ as the space variables and expanded the solution in Fourier series in terms of θ . In this appendix, the axisymmetrical equations will be used, and the results will be compared with those of Jahsman.

Differentiating (3), (4), and (5) with respect to time and using ϕ_t and w_t for $\partial\phi/\partial t$ and $\partial w/\partial t$, respectively, (1) to (5) become

$$\frac{\partial M_r}{\partial r} + \frac{1}{r}(M_r - M_\theta) - Q_r = \alpha \frac{\partial \phi_t}{\partial t} \tag{A.1}$$

$$\frac{\partial Q_r}{\partial r} + \frac{1}{r} Q_r = \beta \frac{\partial w_t}{\partial t} \tag{A.2}$$

$$\frac{\partial M_r}{\partial t} = D\left(\frac{\partial \phi_t}{\partial r} + \frac{\nu}{r}\phi_t\right) \tag{A.3}$$

$$\frac{\partial M_\theta}{\partial t} = D\left(\frac{\phi_t}{r} + \nu \frac{\partial \phi_t}{\partial r}\right) \tag{A.4}$$

$$\frac{\partial Q_r}{\partial t} = \gamma\left(\phi_t + \frac{\partial w_t}{\partial r}\right) \tag{A.5}$$

where

$$\alpha = \frac{\rho h^3}{12}\ , \quad \beta = \rho h, \text{ and } \quad \gamma = k_2^2 G h$$

These constitute a set of linear, first order equations for the variables M_r, M_θ, Q_r, ϕ_t, and w_t. In regions in the physical plane (r,t-plane) where these variables are continuous, we may write

$$dM_r = \frac{\partial M_r}{\partial r} dr + \frac{\partial M_r}{\partial t} dt \qquad (A.6)$$

$$dM_\theta = \frac{\partial M_\theta}{\partial r} dr + \frac{\partial M_\theta}{\partial t} dt \qquad (A.7)$$

$$dQ_r = \frac{\partial Q_r}{\partial r} dr + \frac{\partial Q_t}{\partial t} dt \qquad (A.8)$$

$$d\phi_t = \frac{\partial \phi_t}{\partial r} dr + \frac{\partial \phi_t}{\partial t} dt \qquad (A.9)$$

$$dw_t = \frac{\partial w_t}{\partial r} dr + \frac{\partial w_t}{\partial t} dt \qquad (A.10)$$

Equations (A.1) to (A.10) may be considered as ten algebraic equations for the ten derivatives of the five variables. Solving these equations for $\partial M_r/\partial r$, we obtain

$$\frac{\partial M_r}{\partial r} = \frac{\begin{vmatrix} Q_r - \frac{1}{r}(M_r - M_\theta) & 0 & 0 & 0 & 0 & 0 & 0 & -\alpha & 0 & 0 \\ -\frac{1}{r} Q_r & 0 & 1 & 0 & 0 & 0 & 0 & 0 & 0 & -\beta \\ D\frac{1}{r}\phi_t & 1 & 0 & 0 & 0 & 0 & -D & 0 & 0 & 0 \\ D'\frac{1}{r}\phi_t & 0 & 0 & 0 & 0 & 1 & -D\nu & 0 & 0 & 0 \\ \gamma'\phi_t & 0 & 0 & 1 & 0 & 0 & 0 & 0 & -\gamma & 0 \\ dM_r & dt & 0 & 0 & 0 & 0 & 0 & 0 & 0 & 0 \\ dM_\theta & 0 & 0 & 0 & dr & dt & 0 & 0 & 0 & 0 \\ dQ_r & 0 & dr & dt & 0 & 0 & 0 & 0 & 0 & 0 \\ dw_t & 0 & 0 & 0 & 0 & 0 & 0 & 0 & dr & dt \\ d\phi_t & 0 & 0 & 0 & 0 & 0 & dr & dt & 0 & 0 \end{vmatrix}}{\begin{vmatrix} 1 & 0 & 0 & 0 & 0 & 0 & 0 & -\alpha & 0 & 0 \\ 0 & 0 & 1 & 0 & 0 & 0 & 0 & 0 & 0 & -\beta \\ 0 & 1 & 0 & 0 & 0 & 0 & -D & 0 & 0 & 0 \\ 0 & 0 & 0 & 0 & 1 & -D\nu & 0 & 0 & 0 & 0 \\ 0 & 0 & 0 & 1 & 0 & 0 & 0 & 0 & -\gamma & 0 \\ dr & dt & 0 & 0 & 0 & 0 & 0 & 0 & 0 & 0 \\ 0 & 0 & 0 & 0 & dr & dt & 0 & 0 & 0 & 0 \\ 0 & 0 & dr & dt & 0 & 0 & 0 & 0 & 0 & 0 \\ 0 & 0 & 0 & 0 & 0 & 0 & 0 & 0 & dr & dt \\ 0 & 0 & 0 & 0 & 0 & 0 & dr & dt & 0 & 0 \end{vmatrix}}$$

$$= \frac{(dr)^2 \alpha \left[\gamma (dt)^2 - \beta (dr)^2\right] \left\{ dM_r - \frac{D dt}{r dr} \left[\nu \Phi_t dr + r d\Phi_t + \frac{r Q_r - (M_r - M_\theta)}{\alpha} dt \right] \right\}}{dr \left[D(dt)^2 - \alpha (dr)^2 \right] \left[\beta (dr)^2 - \gamma (dt)^2 \right]}$$

(A.11)

If the distribution of the five variables along a given line is known, this equation and the other nine equations for the remaining derivatives may be obtained and the process of numerical integration may be carried out. This integration procedure fails if the denominator of (A.11) vanishes, which results in the following five physical characteristics

$$\left.\begin{matrix} I^+ \\ I^- \end{matrix}\right\} \quad \frac{dr}{dt} = \pm c_p = \pm \left[\frac{E}{\rho (1 - \nu^2)} \right]^{1/2} \tag{A.12}$$

$$\left.\begin{matrix} II^+ \\ II^- \end{matrix}\right\} \quad \frac{dr}{dt} = \pm h_2 c_2 = \pm h_2 \left(\frac{G}{\rho} \right)^{1/2} \tag{A.13}$$

$$III \quad dr = 0 \tag{A.14}$$

Along the characteristics II^+, II^-, and III, the numerator of (A.11) vanishes identically. Along I^+ and I^-, the vanishing of the numerator upon substitution of $dr/dt = \pm c_p$, yields

$$\left.\begin{matrix} I^+ \\ I^- \end{matrix}\right\} dM_r \mp c_p \frac{\rho h^3}{12} d\Phi_t = \left(r Q_r - M_r + M_\theta \pm \nu c_p \frac{\rho h^3}{12} \Phi_t \right) \frac{dr}{r} \tag{A.15}$$

Thus along I^+ and I^-, (A.15) are the governing equations where only the variables and their total differentials appear. Across all these characteristics, the first derivatives of the five variables may be discontinuous.

Solving (A.1) to (A.10) for any of the other nine derivatives yields the same five physical characteristics. Just as in the case of $\partial M_r/\partial r$, the numerators of the solution of $\partial M_r/\partial t$, $\partial M_\theta/\partial t$, $\partial \phi_t/\partial r$, and $\partial \phi_t/\partial t$, all vanish identially along II^+, II^-, and III. The vanishing of the numerator of each of these solutions along I^+ and I^- also results in (A.15).

The solution of $\partial w_t/\partial t$ is

$$\frac{\partial w_t}{\partial t} = \frac{(dr)^2\left[\alpha(dr)^2 - D(dt)^2\right]\left[dQ_r + Q_r\frac{dr}{r} - \gamma\, dt\left(\phi_t + \frac{\partial w_t}{\partial r}\right)\right]}{dr\left[D(dt)^2 - \alpha(dr)^2\right]\left[\beta(dr)^2 - \gamma(dt)^2\right]} \qquad (A.16)$$

Along I^+, I^-, and III, the numerator of (A.16) vanishes identically; along II^+ and II^- , with $dr/dt = \pm k_2 c_2$, the vanishing of the numerator yields

$$\left.\begin{matrix} II^+ \\ II^- \end{matrix}\right\} \; dQ_r \mp \rho h k_2 c_2\, dw_t = -\left(Q_r \mp \rho h k_2 c_2\, r\, \phi_t\right)\frac{dr}{r} \qquad (A.17)$$

From the solutions of $\partial Q_r/\partial r$, $\partial Q_r/\partial t$, and $\partial w_t/\partial r$, we obtain the same results as from $\partial w_t/\partial t$, i.e., along I^+, I^-, and III, the numerators vanish identically, and along II^+ and II^-, (A.17) is obtained.

The solution of $\partial M_\theta/\partial r$ is

$$\frac{\partial M_\theta}{\partial r} = \frac{D\nu(dt)^2\left[\gamma(dt)^2 - \beta(dr)^2\right]R}{dr\left[D(dt)^2 - \alpha(dr)^2\right]\left[\beta(dr)^2 - \gamma(dt)^2\right]} \qquad (A.18)$$

where

$$R = dM_r + \left[\frac{\alpha}{D}\left(\frac{dr}{dt}\right)^2 - 1\right]\frac{dM_\theta}{\nu} - \alpha\frac{dr}{dt}\,d\phi_t - \left(Q_r - \frac{M_r - M_\theta}{r}\right)dr$$
$$+ \left[\left(\frac{1}{\nu} - \nu\right)D - \frac{\alpha}{\nu}\left(\frac{dr}{dt}\right)^2\right]\frac{\phi_t}{r}\,dt$$

Along II^+ and II^-, the numerator of this vanishes identically; along I^+ and I^- the vanishing of the numerator yields (A.15). In addition, the vanishing of the numerator along III, dr = 0, yields

$$dM_\theta - \nu dM_r = \frac{Eh^3}{12} \Phi_t \frac{dt}{r} \qquad \text{(A.19)}$$

Notice that (A.19) may be obtained directly by combining (A.3) and (A.4) along dr = 0.

The results in this appendix are in agreement with those obtained by Jahsman, except for a slight discrepancy when compared with his (15). It is believed that the last term in the bracket of the second equation of (15) of [6] should have a $\mp$ sign instead of $\pm$; also the second of (15) of [6] should be for his characteristic III and the third of (15) for II.

The characteristic equations (A.15), (A.17), and (A.19) are applicable for continuous fields with possible discontinuity in the second derivatives of ϕ and w and the first derivatives of M_r, M_θ, and Q_r. Across the physical characteristics, discontinuities in the first derivatives of ϕ and w, along with discontinuities in M_r, M_θ, and Q_r, may also exist, but these will not be governed by (A.15), (A.17), and (A.19). Discontinuities in ϕ_r, ϕ_t, w_r, w_t, M_r, M_θ, and Q_r occur when a finite step input (or jump input) in these variables is applied at a particular r. The equations governing the propagation of these discontinuities will be derived below following the general procedure of [7].

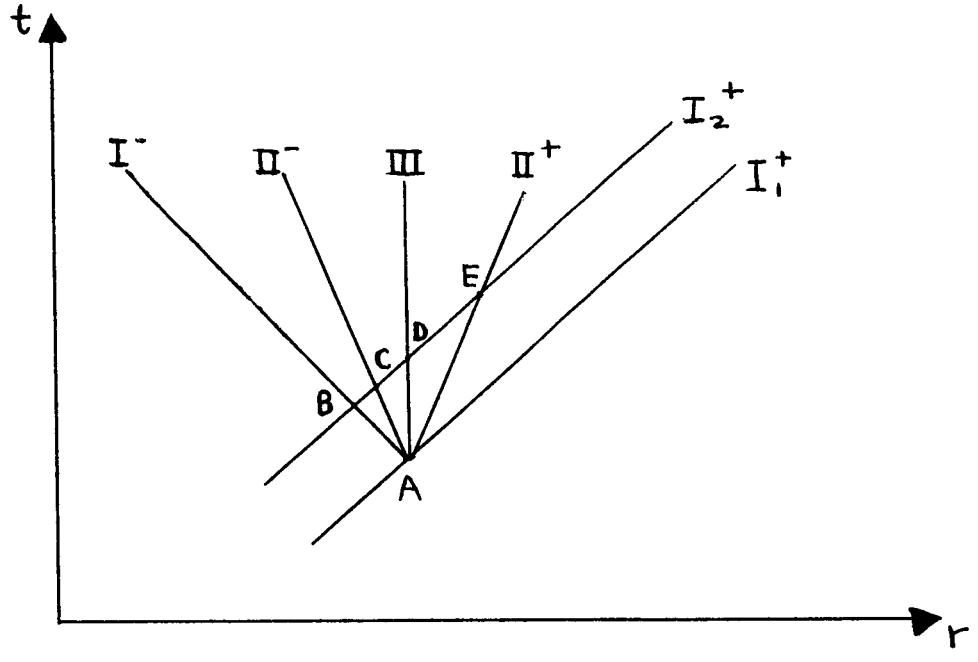

Figure A.1 Discontinuities Propagating Along a I^+ Characteristic

Writing (A.15) with the lower sign along I^- and integrating from points A to B (See Fig. A.1), we have

$$(M_{rB} - M_{rA}) + c_p \alpha (\Phi_{tB} - \Phi_{tA}) = \int_A^B (r Q_r - M_r + M_\theta - \nu c_p \alpha \phi_t) \frac{dr}{r}$$

or

$$\delta M_r + c_p \alpha \delta \Phi_t = 0 \qquad \text{(A.20)}$$

since only bounded values of Q_r, M_r, M_θ, and ϕ_t are being considered the right-hand side vanishes as $dr \to 0$. Similar integrations along II^+, II^-, and III, yield, respectively

$$\delta Q_r - k_2 c_2 \rho h \delta w_t = 0 \qquad \text{(A.21)}$$

$$\delta Q_r + k_2 c_2 \rho h \delta w_t = 0 \qquad \text{(A.22)}$$

$$\delta M_\theta - \nu \delta M_r = 0 \qquad \text{(A.24)}$$

In deriving these three equations, continuity of all variables along I_2^+ has been assumed, thus as a limit,

$$\delta Q_r = Q_{rC} - Q_{rA} = Q_{rE} - Q_{rA} = Q_{rB} - Q_{rA}$$

Equations (A.21) and (A.22) immediately produce

$$\left.\begin{aligned} \delta Q_r &= 0 \\ \delta w_t &= 0 \end{aligned}\right\} \quad \text{across } I^+$$

The variation of the functions δM_r, δM_θ, and $\delta \phi_t$ as they propagate along I^+ is obtained by writing (A.15), with the upper sign, once along I_2^+ and then along I_1^+, and subtracting one from the other. As I_2^+ approaches I_1^+, we have

$$d(\delta M_r) - \alpha c_p d(\delta \phi_t) = (-\delta M_r + \delta M_\theta + \nu c_p \alpha \delta \phi_t)\frac{dr}{r} \qquad \text{(A.24)}$$

Substitution of (A.20) and (A.23) into (A.24) results in

$$\frac{d(\delta M_r)}{\delta M_r} = -\frac{dr}{2r} \qquad \text{(A.25)}$$

which upon integration yields

$$\delta M_r = DA\, r^{-1/2} \qquad \text{(A.26)}$$

where the constant of integration has been taken as DA, consistent with (18). From (A.26), (A.20), and (A.23),

$$\delta M_\theta = \nu DA\, r^{-1/2} \qquad \text{(A.27)}$$

$$\delta \phi_t = -c_p A\, r^{-1/2} \qquad \text{(A.28)}$$

Since we are limited to bounded functions of M_r, M_θ, and ϕ_t, it follows from (3) and (4) that ϕ_r must also be bounded, therefore ϕ is always continuous, or $\delta\phi = 0$. Alternatively, if we limit ϕ to continuous functions, then it follows that M_r, M_θ, ϕ_t, and ϕ_r are always bounded. Writing the equation $d\phi = \phi_r dr + \phi_t dt$ along I_2^+ and

I_1^+, and subtracting one from the other, we obtain

$$0 = \delta\phi_r\, dr + \delta\phi_t\, dt$$

or

$$\delta\phi_r = -\delta\phi_t \frac{dt}{dr} = -\frac{1}{c_p}\,\delta\phi_t \tag{A.29}$$

Therefore,

$$\delta\phi_r = A\, r^{-1/2} \tag{A.30}$$

Repeating this process for discontinuities across I^-, II^+, and II^-, we have the following results:

Across I^+ and I^-

$$\begin{aligned}
&\delta\phi_r = A\, r^{-1/2} \\
&\delta\phi_t = \mp c_p A\, r^{-1/2} \\
&\delta M_r = D A\, r^{-1/2} \\
&\delta M_\theta = \nu D A\, r^{-1/2} \\
&\delta Q_r = \delta w_t = \delta w_r = 0
\end{aligned} \tag{A.31}$$

Across II^+ and II^-

$$\begin{aligned}
&\delta w_r = B r^{-1/2} \\
&\delta w_t = \mp k_2 c_2 B r^{-1/2} \\
&\delta Q_r = k_2^2 G h B r^{-1/2} \\
&\delta\phi_r = \delta\phi_t = \delta M_r = \delta M_\theta = 0
\end{aligned} \tag{A.32}$$

APPENDIX B

Method of Characteristics - Displacement Approach

The method of characteristics as applied to the system of equations (6) and (7) is outlined in this appendix. In regions in the physical plane (r,t-plane) where the variables ϕ_r, ϕ_t, w_r, and w_t, are continuous, we may write

$$\begin{aligned} d\phi_r &= \phi_{rr}dr + \phi_{rt}dt \\ d\phi_t &= \phi_{rt}dr + \phi_{tt}dt \\ dw_r &= w_{rr}dr + w_{rt}dt \\ dw_t &= w_{rt}dr + w_{tt}dt \end{aligned} \tag{B.1}$$

These equations, together with (6) and (7), form a system of six simultaneous equations as follows

$$\begin{aligned} \phi_{rr} - \lambda_1 \phi_{tt} &= F \\ w_{rr} - \lambda_2 w_{tt} &= H \\ dr\,\phi_{rr} + dt\,\phi_{rt} &= d\phi_r \\ dr\,\phi_{rt} + dt\,\phi_{tt} &= d\phi_t \\ dr\,w_{rr} + dt\,w_{rt} &= dw_r \\ dr\,w_{rt} + dt\,w_{tt} &= dw_t \end{aligned} \tag{B.2}$$

where

$$F = \frac{k_2^2 Gh}{D}\left(\phi + \frac{\partial w}{\partial r}\right) + \frac{1}{r^2}\phi - \frac{1}{r}\frac{\partial \phi}{\partial r}$$

$$H = -\frac{1}{r}\left(\phi + \frac{\partial w}{\partial r}\right) - \frac{\partial \phi}{\partial r}$$

$$\lambda_1 = \frac{\rho h^3}{12D}$$

$$\lambda_2 = \frac{\rho}{k_2^2 G}$$

Equations (B.2), in general, may be used to solve for the six second derivatives of ϕ and w. Along certain directions, however, indeterminate solutions for these second derivatives will be obtained from (B.2). These directions will be called characteristic, and lines along these directions will be called the physical characteristics, or simply characteristics. Across these characteristics, the second derivatives of ϕ and w may be discontinuous.

Solving (B.2) for ϕ_{rr}, we have

$$\Phi_{rr} = \frac{\begin{vmatrix} F & 0 & -\lambda_1 & 0 & 0 & 0 \\ H & 0 & 0 & 1 & 0 & -\lambda_2 \\ d\Phi_r & dt & 0 & 0 & 0 & 0 \\ d\Phi_t & dr & dt & 0 & 0 & 0 \\ dw_r & 0 & 0 & dr & dt & 0 \\ dw_t & 0 & 0 & 0 & dr & dt \end{vmatrix}}{\begin{vmatrix} 1 & 0 & -\lambda_1 & 0 & 0 & 0 \\ 0 & 0 & 0 & 1 & 0 & -\lambda_2 \\ dr & dt & 0 & 0 & 0 & 0 \\ 0 & dr & dt & 0 & 0 & 0 \\ 0 & 0 & 0 & dr & dt & 0 \\ 0 & 0 & 0 & 0 & dr & dt \end{vmatrix}}$$

$$= \frac{[\lambda_2(dr)^2 - (dt)^2][\lambda_1 d\Phi_t dt + F(dt)^2 - \lambda_1 d\Phi_r dr]}{[(dt)^2 - \lambda_1(dr)^2][(dt)^2 - \lambda_2(dr)^2]} \qquad (B.3)$$

This function is indeterminate if both numerator and denominator are equal to zero. The vanishing of the denominator yields the following four families of physical characteristics,

$$\left.\begin{matrix} I^+ \\ I^- \end{matrix}\right\} \frac{dr}{dt} = \pm \frac{1}{\sqrt{\lambda_1}} = \pm c_p$$

$$\left.\begin{matrix} II^+ \\ II^- \end{matrix}\right\} \frac{dr}{dt} = \pm \frac{1}{\sqrt{\lambda_2}} = \pm k_2 c_2$$

Along the directions II^+ and II^-, the numerator of (B.3) vanishes identically; along I^+ and I^-, the vanishing of the numerator yields

$$\left.\begin{matrix} I^+ \\ I^- \end{matrix}\right\} d\Phi_t \mp c_p d\Phi_r = \mp c_p \left[\frac{k_2^2 G h}{D}(\phi + w_r) + \frac{\Phi}{r^2} - \frac{\Phi_r}{r}\right] dr \qquad \text{(B.4)}$$

which are called the characteristic equations along $dr/dt = \pm c_p$.

Solution for each of the other five second derivatives gives the same four physical characteristics. The numerator of the solution for w_{rr} is

$$\left[\lambda_1 (dr)^2 - (dt)^2\right]\left[\lambda_2 \, dw_r \, dr - \lambda_2 \, dw_t \, dt - H(dt)^2\right]$$

which vanishes identically along I^+ and I^-, and yields the following characteristic equations along II^+ and II^-,

$$\left.\begin{matrix} II^+ \\ II^- \end{matrix}\right\} dw_r \mp \frac{dw_t}{k_2 c_2} = -\left[\frac{(\phi + w_r)}{r} + \Phi_r\right] dr \qquad \text{(B.5)}$$

The vanishing of the numerators of ϕ_{rt} and ϕ_{tt} give the same results as those from ϕ_{rr}; results from the solutions of w_{rt} and w_{tt} are identical to those from w_{rr}. Equations (B.4) and (B.5) are the

governing equations along the characteristic directions for the variables ϕ, ϕ_r, ϕ_t, w_r, and w_t. By using (A.3), (A.4), and (A.5), it can be shown that (B.4) and (B.5) can be derived from (A.15) and (A.17), respectively.

The equations governing the propagation of discontinuities can be derived by a procedure similar to the stress formulation in Appendix A. Integrating (B.4) along I^- from A to B, (Fig. A.1), we may write

$$(\phi_{t_B} - \phi_{t_A}) + c_p(\phi_{r_B} - \phi_{r_A}) = c_p \int_A^B \left[\frac{k_2^2 Gh}{D}(\phi + w_r) + \frac{\phi}{r^2} - \frac{\phi_r}{r} \right] dr$$

or

$$\delta\phi_t + c_p \delta\phi_r = 0 \qquad \text{(B.6)}$$

The vanishing of the right-hand side when $dr \to 0$, is dependent on the boundedness of ϕ, ϕ_r, and w_r.

Similarly integration along II^- from A to C and II^+ from A to E yields, respectively

$$\delta w_r - \frac{1}{k_2 c_2} \delta w_t = 0 \qquad \text{(B.7)}$$

$$\delta w_r + \frac{1}{k_2 c_2} \delta w_t = 0 \qquad \text{(B.8)}$$

In writing these equations, we must require ϕ, ϕ_r, and w_r to be bounded along II^- and II^+. Equations (B.7) and (B.8) imply that

$$\left.\begin{aligned} \delta w_r &= 0 \\ \delta w_t &= 0 \end{aligned}\right\} \text{ across } \frac{dr}{dt} = +c_p$$

The variation in amplitude of the functions $\delta\phi_t$, $\delta\phi_r$ as they propagate along I^+ is obtained by writing (B.4) with the upper sign along I_2^+ and I_1^+ and subtracting one from the other. As I_2^+ approaches I_1^+, we have

$$d(\delta\Phi_t) - c_\phi d(\delta\Phi_r) = + c_\phi \frac{1}{r} \delta\Phi_r dr \qquad \text{(B.9)}$$

Combining (B.6) and (B.9) and integrating, we obtain

$$\delta\Phi_r = A r^{-1/2}$$

which is identical with the first of (A.31). By similar procedures, all of equations (A.31) and (A.32) may be obtained by the displacement approach. The third of (A.31) is obtained from (A.30), (3) and the condition that ϕ must be continuous, or $\delta\phi = 0$.